Noncanonical roles for Tropomyosin during myogenesis

Jessica Williams, Nathan G. Boin, Juliana M. Valera, and Aaron N. Johnson[1]

Department of Integrative Biology
University of Colorado Denver
Denver, CO 80217

[1]Author for correspondence: aaron.n.johnson@ucdenver.edu

Summary

For skeletal muscle to produce movement, individual myofibers must form stable contacts with tendon cells and then assemble sarcomeres. The myofiber precursor is the nascent myotube, and during myogenesis the myotube completes guided elongation to reach its target tendons. Unlike the well-studied events of myogenesis, such as myoblast specification and myoblast fusion, the molecules that regulate myotube elongation are largely unknown. In *Drosophila*, *hoi polloi (hoip)* encodes a highly-conserved RNA binding protein and *hoip* mutant embryos are largely paralytic due to defects in myotube elongation and sarcomeric protein expression. We used the *hoip* mutant background as a platform to identify novel regulators of myogenesis, and uncovered surprising developmental functions for the sarcomeric protein Tropomyosin 2 (Tm2). We have identified Hoip responsive sequences in the coding region of the *Tm2* mRNA that are essential for Tm2 protein expression in developing myotubes. Tm2 overexpression rescued the *hoip* myogenic phenotype by promoting F-actin assembly at the myotube leading edge, by restoring the expression of additional sarcomeric RNAs, and by promoting myoblast fusion. Embryos that lack *Tm2* also showed reduced sarcomeric protein expression, and embryos that expressed a gain-of-function *Tm2* allele showed both fusion and elongation defects. Tropomyosin therefore dictates fundamental steps of myogenesis prior to regulating contraction in the sarcomere.

Introduction

Nascent myotubes are faced with two major obstacles before they can form functional, contractile myofibers. First, the myotube must elongate over several cell diameters to identify and contact the appropriate tendon cells (Schnorrer and Dickson, 2004). Second, the myotube must express a host of muscle structural proteins and assemble those proteins into contractile sarcomeres (Rui et al., 2010). Although the mechanisms that regulate myotube precursor specification and muscle structural gene transcription have been characterized in detail (Buckingham and Rigby, 2014; Ciglar and Furlong, 2009), the molecules that coordinate myotube elongation are poorly understood.

The genetic tools in *Drosophila* have identified conserved cellular and molecular processes that direct striated muscle development. *Drosophila* somatic muscle is analogous to vertebrate skeletal muscle, and somatic muscle development initiates with the specification of myoblasts known as founder cells, that then fuse with neighboring fusion competent cells to form nascent, multinucleate myotubes (Chen and Olson, 2004; de Joussineau et al., 2012). The nascent myotubes then elongate, activate muscle structural gene expression, attach to tendons, and assemble sarcomeres to form a functional myofiber (Rui et al., 2010; Schejter and Baylies, 2010).

Tropomyosin is a sarcomeric protein that binds thin filament actin to regulate contractions. Outside of the sarcomere, Tropomyosin also directs cytoskeletal dynamics in migratory cells. Membrane protrusions at the leading edge of migrating cells are driven by actin polymerizing proteins in the lamellipodia, and the physical force for cell movement is derived from lamellar expansion (Ponti et al., 2004). Tropomyosins are essential actin stabilizing proteins in the lamella that act in concert with the actin polymerizing proteins at the leading edge, including the Wiskott-Aldrich syndrome proteins (WASP) and the actin-related proteins (ARP)2/3 complex, to drive both normal and metastatic cell migration (Bugyi and Carlier, 2010; Gross, 2013). With respect to myogenesis, the WASP and ARP2/3 protein complexes are essential for myoblast fusion (Baas et al., 2012; Berger et al., 2008; Richardson et al., 2007), and WASP proteins promote myoblast migration (Kawamura et al.,

2004). Although the mechanisms that direct myotube elongation are thought to mimic those of migratory cells (Bongiovanni et al., 2012), the role of Tropomyosin during myotube elongation has not been characterized.

We previously identified the RNA binding protein Hoi Polloi (Hoip) in a screen for regulators of *Drosophila* myotube elongation (Johnson et al., 2013). *hoip* mutant embryos are largely paralytic due to defects in myotube elongation, as well as defects in myoblast fusion and sarcomeric gene expression. The *Drosophila* genome encodes two Tropomyosin isoforms, *Tm1* and *Tm2*, and both isoforms were dramatically reduced in *hoip* embryos. Here we show Tm2 co-localized with F-actin during myotube elongation, and Hoip responsive sequences in *Tm2* mRNA are required for Tm2 protein expression in somatic muscle. Tm2 overexpression rescued *hoip* myogenic defects by restoring F-actin during myotube elongation, by promoting myoblast fusion, and by enhancing the expression of additional sarcomeric proteins. *Tm2* null embryos showed reduced sarcomeric protein expression, and a gain-of-function *Tm2* allele disrupted myotube elongation and myoblast fusion. Tropomyosin is therefore an essential regulator of myogenesis prior to sarcomere assembly.

Results

Tm2 expression and localization suggests a novel function.

hoip^{1} mutant embryos showed two major myogenic phenotypes. A subset of somatic myotubes [including Lateral Longitudinal (LL1), Dorsal Oblique (DO3-5), Lateral Transverse (LT1-4), and Lateral Oblique (LO1)] failed to elongate (Fig. 1A; see Fig. S1A for a diagram of somatic muscle), and sarcomeric RNAs were dramatically down regulated in striated muscles (Johnson et al., 2013). Myoblast fusion was also affected in *hoip*^{1} embryos. A mechanism that could explain the *hoip* mutant phenotype is that Hoip promotes the expression of cytoskeletal regulatory proteins that direct myogenesis. To identify potential Hoip targets, we re-examined our *hoip* RNA-seq data for misregulated transcripts with Gene Ontology (GO) terms associated with cytoskeletal regulation. Twenty-five misregulated transcripts were associated with these GO terms, including *Tm1* and *Tm2*. Tropomyosin protein expression initiated in the somatic mesoderm during founder cell specification and is robustly expressed in elongating myotubes (Fig 1B,C). On the other hand, Mhc expression did not initiate until myotube elongation was largely complete (Fig. 1D). We characterized a third sarcomeric protein, *Z-band alternatively spliced PDZ-motif protein 66,* and found Zasp66 expression did not initiate until St16 (Fig. S1B-D). Thus, the Tropomyosin expression pattern is temporally and spatially consistent with a role for Tropomyosin in myotube elongation, and Tropomyosin expression is temporally distinct from other sarcomeric proteins.

If Tropomyosin is required for myotube elongation, we reasoned that Tropomyosin would co-localize with F-actin at the myotube leading edge. Embryos harboring an endogenous *Tm2* protein trap (hereafter *Tm2*^{GFP}, Buszczak et al., 2007) were labeled for GFP and F-actin. Tm2^{GFP} co-localized with F-actin at the myotube leading edge throughout elongation and during muscle attachment (Fig. 1E-G). Tm2 subcellular localization further suggested that Tropomyosin is required for myotube elongation, and that Tm2 interacts with F-actin prior to sarcomere assembly.

Tm2 protein expression requires Hoip.

hoip expression is not ubiquitous, and within the embryonic mesoderm *hoip* expression is restricted to the striated muscle lineages and the fat body (Johnson et al., 2013). The human Hoip orthologue NHP2L1 performs multiple cellular functions that include pre-mRNA splicing and ribosomal RNA processing (Schultz et al., 2006). In fact, the crystal structure of NHP2L1 bound to the spliceosomal RNA U4 has been solved (Liu et al., 2007). NHP2L1 also shows sequence similarities to the archaeal ribosomal protein L7Ae (Kuhn et al., 2002), suggesting that Hoip could be a ribosomal component. Our previous studies showed Hoip localizes to both the nucleus and the cytoplasm of elongating myotubes (Johnson et al., 2013). Hoip could thus be required for pre-mRNA splicing, mRNA nuclear export, mRNA stability and localization, or mRNA translation.

To distinguish among these possibilities, we designed an *in vivo* splicing assay in which a series of *Tm2* genomic constructs (*Tm2GFP#1-3*) were cloned upstream of a C-terminal GFP tag in a UAS transgenic vector (Fig. 2A, S2A). For each construct, GFP expression requires correct splicing of the encoded transcript. We considered the possibility that excessive overexpression of the *Tm2* constructs would be sufficient to detect GFP expression in *hoip*^{1} embryos. To increase the sensitivity of the assay, we used random transposition to generate both low-level and high-level expressing lines for a comparative analysis.

The *Tm2* genomic constructs were expressed in developing somatic muscles with *RP298.gal4.* As a control for *RP298.gal4* activity in *hoip*^{1} embryos, we assayed somatic muscle GFP expression from *UAS.τGFP*. *RP298.gal4* is also active in the salivary gland, so salivary gland fluorescence was used to normalize somatic muscle transgene expression. WT and *hoip*^{1} muscles produced comparable levels of τGFP in somatic muscles (Fig. 2B,C; *hoip*^{1} τGFP fluorescence = 117.9% of WT, n=42). However, *hoip*^{1} embryos that expressed the low-level *Tm2-GFP* constructs produced only a fraction of WT GFP fluorescence in

somatic muscles (Fig 2D-J,P; *Tm2-GFP#1*: 18.0%, n=36; *Tm2-GFP#2*: 24.0%, n=48; *Tm2-GFP#3*: 24.7% n=48). On the other hand, *hoip*^{1} embryos that expressed the high-level *Tm2-GFP* constructs in somatic muscles showed GFP fluorescence that was comparable to WT embryos (Fig. 2L-N, S2EB-G; *Tm2-GFP#1*: 89.3%, n=66; *Tm2-GFP#2*: 167.6%, n=48; *Tm2-GFP#3*: 137.9% n=36). In fact, some *hoip* muscles showed higher Tm2-GFP fluorescence than WT muscles. We attribute this to the fact that *hoip* muscles are smaller than WT muscles, and the GFP signal is concentrated over a smaller area. Our splicing assays showed Hoip regulates Tm2 protein expression during myogenesis, but surprisingly suggest that Hoip is not necessary for pre-mRNA splicing.

Hoip promotes Tm2 protein expression through a splicing-independent mechanism.

To test the possibility that Hoip facilitates Tm2 protein expression after pre-mRNA splicing, we generated stable insertions of a C-terminal GFP-tagged *Tm2-cDNA* under UAS control. Similar to the intron-containing constructs, *hoip*^{1} embryos that expressed a low-level *Tm2-cDNA.GFP* showed reduced Tm2-GFP expression compared to WT embryos (Fig. 2K,P; 52.1% n=48), and *hoip*^{1} embryos that expressed a high-level *Tm2-cDNA.GFP* construct showed WT levels of Tm2-GFP expression (Fig. 2O,P; 125.0%, n=42). Thus Tm2-GFP expression from a cDNA also required Hoip, which further argues that Hoip regulates Tm2 expression through a splicing independent mechanism.

To confirm these observations, we generated Flag-tagged *Tm2* constructs for expression in *Drosophila* S2 cells (Fig. 2Q). S2 cells co-transfected with Hoip and either the *Tm2* genomic constructs or the *Tm2* cDNA construct produced more Tm2 protein than cells co-transfected with the *Tm2* constructs and a control vector (Fig. 2Q). Importantly, cells transfected with Hoip did not show enhanced expression of β-tubulin, which argues that Hoip is not a global regulator of protein expression. We could not detect Tm2-Flag protein expression from *Tm2#3*, which suggests that alternative exon 5a is exclusively selected in S2 cells (data not shown). The *Tm2#2* genomic construct contains three exons and two

introns, and cells transfected with Hoip did not show enhanced splicing of *Tm2#2* transcripts compared to control transfected cells by quantitative real-time PCR (qPCR; Fig. 2R). These *in vitro* experiments confirmed that Hoip regulates Tm2 protein expression through a splicing independent mechanism.

Hoip promotes protein expression after Tm2 *mRNA nuclear export*

To understand if Hoip is required for *Tm2* mRNA nuclear export, we assayed *Tm2* mRNA localization by *in situ* hybridization. WT embryos showed robust *Tm2* expression in all somatic muscles, whereas *hoip*^{1} embryos expressed *Tm2* at low-levels in the dorsal and ventral muscle groups, but not in the lateral muscles (Fig. 3A,B). *hoip*^{1} embryos that expressed the low-level *Tm2-GFP#3* construct showed significant *Tm2* mRNA in the somatic muscle cytoplasm, but Tm2-GFP protein was largely undetectable (Fig. 3C). However, *hoip*^{1} embryos that expressed the high-level *Tm2-GFP#3* showed robust Tm2-GFP protein expression in somatic muscles (Fig. 3D). *Tm2* mRNAs are therefore exported from the nucleus in *hoip*^{1} embryos, but the transcript is not robustly translated when expressed at low levels.

Hoip acts on the Tm2 *coding region to promote protein expression*

RNA binding proteins typically act outside of the coding region to regulate mRNA translation and stability. However, our *Tm2* transgenic constructs contained exogenous 5' and 3' untranslated regions (UTRs). We suspected that Hoip must act within the coding region to regulate Tm2 protein expression. To identify Hoip responsive sequences, we co-transfected S2 cells with Hoip and a series of *Tm2* coding region fragments. These assays showed that the 5' 260bp of the *Tm2* mRNA are Hoip responsive (Fig. S3). We deleted these sequences from the *Tm2* cDNA (*Tm2-ΔcDNA*), and found S2 cells transfected with *Tm2-ΔcDNA* alone did not produce as much Tm2 protein as cells transfected with full-length *Tm2-cDNA* (Fig. 3E). In addition, cells co-transfected with Hoip and *Tm2-ΔcDNA* did not

express robust Tm2Δ protein (Fig. 3E). To confirm these observations *in vivo*, we expressed *Tm2-ΔcDNA.GFP* with *RP298.gal4.* Although Tm2Δ.GFP protein was clearly visible in the salivary gland, Tm2Δ.GFP protein was largely undetectable in somatic muscle (Fig. 3F-H). In addition, *Tm2-ΔcDNA.GFP* transcripts were present in the cytoplasm of somatic muscles at levels comparable to full length *Tm2-cDNA.GFP* transcripts (Fig. 3I,J). Hoip therefore acts within the *Tm2* coding region to direct Tm2 protein expression in somatic muscles.

Tm2 *rescues myotube elongation defects in* hoip *embryos.*

Control *hoip*^{1} embryos that expressed τGFP in the somatic musculature showed a dramatic reduction in the number of completely elongated LL1 (16.1%, n=57) and LT1-3 (3.9%, n=147) muscles compared to WT embryos (Fig. 4A,B,O). *hoip*^{1} embryos that expressed low-level *Tm2-GFP* constructs in the somatic musculature showed myotube elongation defects similar to *hoip*^{1} embryos that expressed τGFP (Fig. 4C-H; *Tm2-GFP#1*: LL1=16.1%, LT1-3=15.3%; *Tm2-GFP#2*: LL1=26.7%, LT1-3=28.2%; *Tm2-GFP#3*: LL1=11.1%, LT1-3=6.8%). Remarkably, *hoip*^{1} embryos that expressed high-level *Tm2-GFP* constructs in the somatic musculature showed a significant recovery in the number of elongated myotubes compared to control *hoip*^{1} embryos (Fig. 4I-N; *Tm2-GFP#1*: LL1=50.4%, n=71 LT1-3=39.1%, n=213; *Tm2-GFP#2*: LL1=59.8% n=67, LT1-3=55.4%, n=204; *Tm2-GFP#3*: LL1=69.5% n=53, LT1-3=14.6%, n=159).

To extend this observation, we assayed Tm2-GFP expression and myotube elongation in embryos with two copies of the low-level *Tm2-GFP* insertions. *hoip*^{1} embryos with two copies of the low-level expressing *Tm2-GFP* genomic constructs produced more Tm2-GFP than *hoip*^{1} embryos with just a single copy (Fig. S4A-I; *Tm2-GFP#1*: 497.6%, n=48; *Tm2-GFP#2*: 703.8%, n=48; *Tm2-GFP#3*: 599.4%, n=66; *Tm2-cDNA.GFP*: 161.3%, n=66; percent relative to single copy). In addition, *hoip*^{1} embryos with two copies of each *Tm2-GFP* showed a significant recovery in the number of elongated myotubes compared to *hoip*^{1} embryos with just a single copy (Fig. S4I; *Tm2-GFP#1*: LL1=336.5%, n=62, LT1-

3=290.0%, n=186; *Tm2-GFP#2*: LL1=304.3%, n=66, LT1-3=155.9% n=171; *Tm2-GFP#3*: LL1=598.0%, n=74, LT1-3=169.3%, n=222; *Tm2-cDNA.GFP*: LL1=251.7%, n=73, LT1-3=326.3%, n=219). Tm2 therefore promotes myotube elongation in *hoip*^{1} embryos.

Tm2 *regulates F-actin during myotube elongation.*

Tropomyosin localizes to F-actin in the lamella of migratory cells, and the contractile F-actin/myosin lamellar network provides the physical force to drive cell movement (Ponti et al., 2004; Ridley et al., 2003). Since Tm2 co-localized with F-actin during myotube elongation (Fig. 1E,F), we predicted that Tm2 regulates F-actin at the myotube leading edge. Compared to WT embryos (Fig. 5A-C,P; St 12 DO5=9.5; St 13 DO5=14.9; St 15 DO5=9.9; arbitrary units, n≥12 myotubes per stage), *hoip*^{1} embryos showed a significant decrease in leading edge F-actin (Fig. 5D-F,P; St 12 DO5=3.9; St 13 DO5=3.5; St 15 DO5=4.5; n≥18). However, *hoip*^{1} embryos that expressed the high-level *Tm2-GFP#3* assembled significantly more leading edge F-actin than *hoip*^{1} embryos (Fig. 5G-I,P; St 12 DO5=5.0; St 13 DO5=7.2; St 15 DO5=9.0; n≥21). Thus, Tm2 promotes F-actin assembly at the myotube leading edge.

Tm2 regulates actin expression.

Similar to vertebrates, *Drosophila* embryos express muscle-specific actin isoforms. *Actin57B* (*Act57B*) is a component of somatic muscle thin filaments, and *Act57B* expression initiates as early as St11 (Kelly et al., 2002). Compared to WT embryos, *Act57B* mRNA levels were dramatically reduced in *hoip*^{1} embryos (Fig. 5J,K; S5A,B), and *hoip*^{1} embryos that expressed *Tm2-GFP#3* showed improved *Act57B* expression in somatic muscles (Fig. 5L, S5C). Importantly, the probe used to detect *Act57B* binds to the highly divergent 3'UTR that distinguishes it from other actin isoforms (Kelly et al., 2002). To understand how Hoip and Tm2 regulate *Act57B*, we used the minimal reporter gene *Act57B.-593/+2.nlacZ* to assay transcriptional activity (Kelly et al., 2002). Compared to WT embryos (Fig. 5M,Q S5D; St13=6.7; St16=8.4; arbitrary units, n≥150 nuclei per stage), *Act57B.-593/+2* reporter

expression was reduced in *hoip*^{1} embryos (Fig. 5N,P S5E; St13=2.7; St16=5.7; n≥150). *hoip*^{1} embryos that expressed *Tm2-GFP#3* showed a slight, yet significant, increase in reporter gene expression compared to *hoip*^{1} embryos (Fig. 5O,P S5F; St13=4.6; St16=6.9; n≥150).

Tm2 promotes sarcomere assembly.

F-actin performs multiple functions during myogenesis beyond myotube elongation. For example, F-actin stress fibers are thought to provide the template for sarcomere assembly (Friedrich et al., 2012). Since Tm2 restored *Act57B* transcription and leading edge F-actin in *hoip*^{1} embryos, we suspected that Tm2 might also regulate F-actin during sarcomere assembly. By St17, WT somatic muscles have assembled thin filament F-actin. However, F-actin was absent from the somatic muscles of *hoip*^{1} embryos and *hoip*^{1} embryos that expressed the low-level *Tm2-GFP#3* (Fig. S5H,N). Strikingly, somatic muscles of *hoip*^{1} embryos that expressed the high-level *Tm2-GFP#3* assembled thin filament F-actin (Fig. S5I). Tm2-GFP also localized to sarcomeres in WT St17 embryos (Fig. S5J,L). Consistent with our F-actin results, Tm2-GFP from the high-level expressing line localized to sarcomeres in *hoip*^{1} embryos whereas Tm2-GFP from the low-level expressing line did not (Fig. S5K,M). It is possible that the low-level expressing line did not produce enough Tm2-GFP for us to detect sarcomeric localization in *hoip*^{1} embryos. However, these embryos also lacked thin filaments so the minimal Tm2-GFP produced likely lacked a substrate for localization. In either case, high-levels of Tm2 restored sarcomere assembly in *hoip*^{1} embryos.

Tm2 *regulates sarcomeric protein expression.*

Knockdown of individual sarcomeric proteins can disrupt sarcomere assembly (Rui et al., 2010). We had previously shown that sarcomeric RNAs were down regulated in *hoip*^{1} embryos at St12-13, and that Mhc protein expression was greatly reduced in St16 *hoip*^{1}

embryos (Johnson et al., 2013). Since Tm2 restored sarcomere assembly in *hoip*^{1} embryos, we expected that Tm2 would also promote the expression of sarcomeric RNAs. Compared to WT embryos, St17 *hoip*^{1} embryos showed reduced expression of *Act57B* (Fold Change=0.44; Fig. 5Q), α-actinin (*Actn*, FC=0.49), *Mhc* (FC=0.38), *Myosin light chain 1* (*Mlc1*, FC=0.52), *Mlc2* (FC=0.16), *TroponinC 47D* (*TpnC47D*, FC=0.42), and *Tm2* (FC=0.61). *hoip*^{1} embryos that expressed *Tm2-GFP#3* showed improved sarcomeric RNA abundance (*Act57B* FC=1.2, *Actn* FC=1.5, *Mhc* FC=1.7, *Mlc1* FC=2.4, *Mlc2* FC=1.9, *TpnC47D* FC=1.9, *Tm2* FC=3.4) compared to *hoip*^{1} embryos (FIG. 5Q). Consistent with these qPCR results, Mhc protein expression, *Mhc* mRNA expression, and *TpnC47D* mRNA expression were also restored in *hoip*^{1} somatic muscles that expressed *Tm2-GFP#3* (Fig. 6A-I).

Tm2 promotes myoblast fusion in hoip *embryos.*

In addition to myotube elongation and sarcomere assembly, F-actin plays a key role in myoblast fusion (Schejter and Baylies, 2010). Our *Act57B* reporter gene experiments showed *hoip*^{1} embryos that expressed *Tm2-GFP#3* contained more lacZ positive nuclei than *hoip*^{1} embryos (Fig. 5N,O). This result suggested that Tm2 promotes myoblast fusion in *hoip*^{1} embryos. The reporter gene *RP298.nlacZ* is expressed in muscle founders, and subsequently in nascent myotubes, and can be used to measure myoblast fusion. *hoip*^{1} embryos that expressed *Tm2-GFP#3* showed more lacZ positive myonuclei than *hoip*^{1} embryos (Fig. 6J). Importantly, myonuclei number in the DO2 muscle was reduced in *hoip*^{1} embryos compared to control embryos, even though the DO2 muscle often elongates (Fig. 6K,L; WT=9.5 DO2 nuclei, *hoip*^{1}=2.5, n≥28). *hoip*^{1} embryos that expressed *Tm2-GFP#3* showed an increased number of DO2 myonuclei compared to *hoip*^{1} embryos (Fig. 6M, 4.6 nuclei/DO2, n=30). Tm2 therefore promotes myoblast fusion in *hoip*^{1} embryos.

Muscle size does not dictate sarcomeric gene expression.

One mechanism that could explain Tm2-mediated gene expression is that Tm2 regulates muscle size, and muscle size in turn dictates sarcomeric gene expression. To test this possibility we normalized Mhc and Tropomyosin protein expression to somatic muscle size, which we refer to as the expression index. The expression index for Mhc and Tropomyosin was significantly reduced in *hoip*^{1} embryos compared to controls. *hoip*^{1} embryos that expressed *Tm2-GFP#3* showed a significantly greater Mhc and Tropomyosin expression index than *hoip*^{1} embryos (Fig. 6J). Therefore, the difference in Mhc expression between *hoip*^{1} and *hoip*^{1} *Tm2-GFP#3* rescued embryos is not simply due to an increase in muscle size.

Tropomyosin regulates Mhc expression.

Our rescue studies showed that Tm2 promotes myoblast fusion, myotube elongation, and sarcomeric gene expression in *hoip*^{1} embryos. To further characterize the function of Tm2 during myogenesis, we generated a *Tm2* null mutation (*Tm2*$^{\Delta 8\text{-}261}$). The *Drosophila* genome encodes only two Tropomyosin isoforms, *Tm1* and *Tm2*, and both isoforms are deleted by *Df(3R)BSC741.* Using qPCR, we confirmed St17 *Tm2*$^{\Delta 8\text{-}261}$ homozygous embryos and St17 *Tm2*$^{\Delta 8\text{-}261}$*/Df(3R)BSC741* transheterozygous embryos did not express *Tm2* (Fig. S6A). In addition, these embryos showed reduced *Act57B* expression compared to control embryos (Fig. S6A, FC=0.29 and 0.31), and *Act57B* expression could be partially restored in *Tm2*$^{\Delta 8\text{-}261}$ embryos that expressed *Tm2* under the control of *RP298.gal4* (Fig. S6A, FC=0.65). The remaining sarcomeric RNAs were expressed at near WT levels in *Tm2* mutant embryos. Surprisingly, myotube elongation was largely unaffected in *Tm2*$^{\Delta 8\text{-}261}$*/Df(3R)BSC741* embryos, but a subset of transheterozygous embryos showed defects in LT1-3 or LL1 morphogenesis in at least one segment (25%, n=12; Fig. 7A,B). *Tm2*$^{\Delta 8\text{-}261}$*/Df(3R)BSC741* embryos also showed a significant reduction in the Mhc expression index compared to

controls but somatic muscle size was unaffected (Fig. 7I). *Tm2*$^{\Delta 8\text{-}261}$ embryos that expressed *Tm2* showed improved LT1-3 and LL1 morphogenesis (14% of embryos with elongation defects, n=14), and improved Mhc expression compared to transheterozygous embryos (Fig. 7C,I).

A dominant Tm2 allele disrupts myotube elongation.

One explanation for the lack of a strong elongation phenotype in *Tm2* embryos is that *Tm2* is maternally contributed. Using qPCR and immunohistochemistry, we confirmed there is a maternal contribution of both *Tm1 and Tm2* mRNAs (Fig. S6B-F). However, females with *Tm2*$^{\Delta 8\text{-}261}$ or *Df(3R)BSC741* homozygous mutant germ lines did not lay eggs. Previous studies showed *Tm1* is required for border cell migration in the ovary (Kim et al., 2011), which suggested Tropomyosin performs essential functions in the germ line. Our results further argue that *Tm1* and *Tm2* are essential for oogenesis.

To further investigate a role for Tm2 during myotube elongation, we generated a dominant *Tm2* allele. The human genome encodes 4 Tropomyosin isoforms (TPM1-4), and congenital myopathies have been associated with dominant Tropomyosin mutations (Marttila et al., 2014; Olson et al., 2001). Tropomyosin is a coiled-coil protein comprised of seven pseudo-repeat domains, and each domain contains an α-zone that interacts with F-actin when muscle is relaxed (Marttila et al., 2014). Several dominant Tropomyosin mutations occur in α-zone residues that are conserved between humans and *Drosophila*, including E54K (Fig. S2). We hypothesized that the E54K mutation would disrupt Tropomyosin function in a dominant fashion, and expressed *Tm2*^{E54K}*-GFP* during myotube elongation with *RP298.gal4*. Otherwise WT embryos that expressed *Tm2*^{E54K}*-GFP* in developing somatic muscles showed a significant reduction in the percent of completely elongated myotubes (Fig.7D-F,J; *line#1*: LL1=75.0%, LT1-3=80.6%; *line#2*: LL1=76.4%, LT1-3=81.3%) and in the number of DO2 nuclei (Fig. 7G,H) compared to embryos that expressed WT *Tm2.GFP*.

These studies further demonstrate that Tm2 is required for myotube elongation and myoblast fusion.

Discussion

Our study has revealed a novel function for Tm2 during myogenesis. Functional rescue experiments showed *Tm2* is epistatic to *hoip* and that Hoip regulates Tm2 protein expression via the coding region. Although Tropomyosins are known regulators of actin dynamics in migratory cells, we found that Tm2 regulates F-actin levels during myotube elongation and sarcomere assembly. In addition, Tm2 promoted myoblast fusion in *hoip*^{1} embryos and regulated Mhc protein expression. To our knowledge, this is the first study to show that Tropomyosins regulate muscle development prior to sarcomere assembly. Lastly, myotubes that expressed the gain-of-function allele *Tm2*^{E54K} showed both fusion and elongation defects. This finding may have important implications in understanding Tropomyosin-related myopathies.

Post-transcriptional regulation of sarcomeric mRNAs

Tm2 protein expression is Hoip dependent, and sequences in the 5' end of the *Tm2* coding region are required for Tm2 expression in somatic muscles (Fig. 3E-J). Hoip orthologues direct spliceosome assembly (Schultz et al., 2006), and we had previously shown that an *Mhc* cDNA restored Mhc protein expression in *hoip* embryos. These findings suggested that Hoip regulates splicing, so we were surprised to discover that Hoip is not required for *Tm2* pre-mRNA splicing or *Tm2* mRNA nuclear export. However, our experiments with *Mhc* and *Tm2* cDNAs did produce similar results. In the case of *Mhc*, we detected Mhc protein expression in *hoip* embryos homozygous for the *Mhc* transgene. In the case of *Tm2*, a high-level expressing insertion or two copies of a low-level insertion produced near WT levels of Tm2.GFP in *hoip* embryos (Fig. 2P, S4). These data argue that

Hoip promotes robust protein expression from endogenous mRNAs, but this requirement can be overcome in *hoip* embryos when the transcripts are overexpressed.

Despite these similarities, Tm2 performs a distinct functional role to enhance sarcomeric protein expression. *Tm2* rescued Mhc protein expression in *hoip* embryos (Fig. 6C), but *Mhc* did not rescue Tropomyosin expression (Johnson et al., 2013). In fact, several sarcomeric mRNAs were enriched in *hoip* embryos that expressed high levels of *Tm2.GFP* (Fig. 5Q). Thus, negative regulation of sarcomeric mRNAs is not simply offset by overexpressing any sarcomeric mRNA. *Tm2* mutant embryos also showed reduced Mhc protein expression (Fig. 7B), but *Mhc* mRNA levels were unaffected (Fig. S6A). Our results demonstrate that Tm2 performs a specific regulatory function, which is distinct at least from Mhc, to promote sarcomeric protein expression. Although Tm2.GFP ameliorated multiple myogenic defects in *hoip* embryos, Tm2.GFP was not sufficient to completely restore myogenesis. This incomplete rescue could be due to a number of factors including the spatial and temporal onset of *Tm2.GFP* expression or that Hoip has at least one additional target mRNA required for myogenesis.

Importantly, Tm2 regulates Mhc expression independent of muscle size (Fig. 6J, 7I). Muscle size is thought to be dependent in part on myoblast fusion (Schejter and Baylies, 2010), and we do see a correlation between myonuclei number and muscle size in St16 embryos (Fig. 6J). Tm2.GFP promoted myoblast fusion in *hoip* embryos (Fig. 6K-L), and $Tm2^{E54K}$ reduced myoblast fusion when expressed in nascent myotubes (Fig. 7G,H). It is possible that Tm2 regulates sarcomeric protein expression by promoting myoblast fusion, which would increase the number of sarcomeric loci, and in turn transcription of sarcomeric genes. However, the Mhc expression index is significantly different between embryos with reduced muscle size and myonuclei number (Fig. 6J). Although we cannot absolutely rule out the possibility that sarcomeric gene transcription contributes to the phenotypes we have reported, it is clear that muscle size, myonuclei number, and gene transcription alone do not account for Tm2-mediated regulation of sarcomeric protein expression.

The role of F-actin during myogenesis

In migratory cells, adhesions with the extracellular matrix form and disassemble at the junction of the lamellipodia and the lamella (Ponti et al., 2004). Actomyosin contractions in the lamella use these adhesion sites to move the cell forward. The lamella is characterized by discrete foci of actin polymerization and depolymerization (Ponti et al., 2004). Migrating epithelial cells that overexpress TPM1 lacked a lamellipodia, but showed rapid migration. Mechanistically, TPM1 overexpression concentrated F-actin and myosin II to the lamella and produced more cellular adhesions (Gupton et al., 2005). A similar cellular mechanism appears to direct myotube elongation. Like TPM1 (Gupton et al., 2005), Tm2 localized to punctate foci near the leading edge (Fig. 1E-G). These foci may reflect sites of Tm2-mediated actomyosin contractions. Since both TPM1 and Tm2 promote F-actin assembly at the leading edge membrane, the cellular mechanism of myotube elongation likely parallels that of migratory cells. The actomyosin network also directs myoblast fusion (Kim et al., 2015). Here, actomyosin tension in the founder cell promotes pore formation at the fusogenic synapse. It will be interesting to see if Tm2 directs the assembly or even the function of the actomyosin network to promote myoblast fusion.

Although we established that Hoip regulates Tm2 through a largely post-transcriptional mechanism, *Act57B.-593/+2* reporter gene expression was reduced in *hoip*^{1} embryos (Fig. 5P), and restored in *hoip*^{1} embryos that expressed *Tm2.GFP*. Accordingly, leading edge F-actin and thin filament F-actin were down regulated in *hoip*^{1} embryos, and rescued by Tm2.GFP (Fig. 5P, S5). The only known molecular function of Tropomyosins is to bind F-actin, so transcriptional regulation of *Act57B* is most likely indirect. F-actin polymerization initiates a feedback loop that drives actin transcription in some contexts (Mokalled et al., 2010), so the changes in *Act57B* transcription we observed are likely a downstream effect of reduced F-actin levels.

Redundancy, compensation, and maternal contribution of Tropomyosin isoforms

Both *Tm1* and *Tm2* are expressed in developing somatic muscles (Fisher et al., 2012), and we confirmed these are the only Tropomyosin encoding genes in the *Drosophila* genome by BLAST analysis. *Tm1* mRNA was enriched in *Tm2* mutant embryos at St11 and St12 (Fig. S6B; F.C=3.1, 2.1), but not at St17 (F.C=0.75). These data argue that *Tm1* compensates for *Tm2* in *Tm2* null embryos at the onset of zygotic transcription. Similarly, *Tm1* mRNA was enriched in *hoip* embryos (Fig. 5Q; F.C=5.0), and reduced in *Tm2.GFP* rescued *hoip* embryos (F.C=2.5). However, elevated *Tm1* levels alone were not sufficient to induce Tropomyosin protein expression in *hoip* embryos, whereas high-level *Tm2.GFP* mRNA produced significant levels of Tm2.GFP protein (Fig. 2L-O, 5Q). Hoip is therefore required for the expression of both Tropomyosin protein isoforms, but different mechanisms appear to direct Tm1 and Tm2 protein expression in somatic muscle.

The modest *Tm2* zygotic phenotype we characterized is consistent with other maternally contributed genes that regulate myogenesis. For example, *rho* and *rok* single mutant embryos develop normal somatic muscles whereas *rho, rok* double mutant embryos show myoblast fusion defects (Kim et al., 2015). Although the maternal contribution of *Tm1* and *Tm2* produced only a fraction of WT transcript levels (Fig. S6B), *Df(3R)BSC741* embryos showed robust Tropomyosin expression during myotube elongation and this expression persisted through St16 (Fig. S6C-F). In contrast, a majority of somatic muscles failed to express Tropomyosin protein in *hoip* mutant embryos (Fig. 6B). Thus, maternally contributed *Tm1/2* can be translated in the presence of Hoip to direct largely normal myogenesis.

Tropomyosin alleles are associated with myopathies

Dominant mutations in *TPM1, TPM2, and TPM3* are associated with congenital myopathies (Marttila et al., 2014) and cardiomyopathies (Karibe et al., 2001; Olson et al., 2001). The *TPM1* E54K allele was identified in patients with dilated cardiomyopathy and *in*

vitro thin filament reconstitution experiments show the E54K protein over inhibits actomyosin interactions, which decreases force generation during systolic contraction (Bai et al., 2012). Our *Tm2* E54K allele disrupted myogenesis (Fig. 7D-F), which argues that Tm2-mediated actomyosin contractions are indeed required for myotube elongation. A second *TPM1* allele, E40K, also interrupts actomysosin contractions (Bai et al., 2012), and *TPM2* E41K is associated with congenital myopathies (Marttila et al., 2014). This raises the possibility that myotube elongation is affected in patients with *TPM2*-associated congenital myopathies. It will be of particular interest to characterize additional Tropomyosin alleles *in vivo* to better understand the disease mechanisms that underlie these myopathies.

Acknowledgements

We thank Richard Cripps for reagents, Mayssa Mokalled for insights and discussions throughout this study and for critical reading of the manuscript, and Brenna Clay for assistance with embryology. ANJ was supported by a Scientist Development Grant (12SDG12030160) from the American Heart Association, and by a Webb-Waring Biomedical Research Award from the Boettcher Foundation.

Author Contributions

J.W., N. G. B., J. M. V., and A.N.J. designed and performed experiments. A.N.J prepared the manuscript.

Materials and Methods

Drosophila *Genetics*

The stocks used in this study were *hoip*^{1} (Johnson et al., 2013), *P{Gal4-kirre*^{rP298}*}* and *P{lacZ-kirre*^{rP298}*}* (Nose et al., 1998), *P{PTT-GC}Tm2*^{ZCL2456} and *P{PTT-GA}Zasp66Z*^{CL0663} referred to as *Tm2*^{GFP} and *Zasp66*^{GFP} protein traps *(Buszczak et al., 2007), P{Act57B-lacZ.-593+2} (Kelly et al., 2002), P{UAS-mCD8.ChRFP}, P{UAS-mCD8.eGFP}, P{UAS-τGFP}, Df(3R)BSC741, P{neoFRT}82B,* and *P{ovoD1-18}3R* (Bloomington Stock Center). *Cyo, P{Gal4-Twi}, P{2X-UAS.eGFP}; Cyo, P{wg.lacZ}; and TM3, P{Gal4-Twi}, P{2X-UAS.eGFP}* balancers were used to identify homozygous embryos.

Tm2 genomic transgenes were constructed by cloning PCRproducts genomic DNA or a cDNA (RE15528) into pEntr (Life Technologies), and then recombined into a destination vectors (TWG and AWG) as described (http://emb.carnegiescience.edu/labs/murphy/Gateway%20vectors.html). Transgenic insertions were generated by standard methods (Rainbow Transgenic Flies, Inc.). *Tm2-ΔcDNA* deletion constructs were generated by PCR sewing as described (Johnson et al., 2013). Entry clones were fully sequenced.

The *Tm2*$^{\Delta 8\text{-}261}$ allele was generated as described (Gratz et al., 2013), and homozygous embryos were sequenced to confirm the *Tm2*$^{\Delta 8\text{-}261}$ mutation. Germ line clones were made by standard methods.

Immunohistochemistry and in situ *Hybridization*

Antibodies used include α-MHC (Kiehart and Feghali, 1986), α-Tropomyosin (Abcam, MAC141), and α-GFP (Torrey Pines Laboratories). HRP-conjugated secondary antibodies and the TSA system (Molecular Probes) were used to detect primary antibodies. Antibody staining and *in situ* hybridization were performed as described (Johnson et al., 2013). RE15528 and LP10264 were used as templates for the *Tm2* and *TpnC47D in situ* probes, respectively. *Mhc* and *Act57B* probes were generated from the templates described

(Johnson et al., 2013; Kelly et al., 2002). Texas red-conjugated phalloidin (Molecular Probes) was used to detect F-actin in fixed, hand devitellinated embryos.

Imaging and fluorescence quantification

Images were generated with an LSM700 confocal microscope (Zeiss). Control and mutant embryos were prepared and imaged in parallel where possible. Confocal imaging parameters were maintained between genotypes throughout the study. Normalized expression was calculated as mean fluorescence intensity over an entire DO2 muscle relative to salivary gland fluorescence (Tm2-GFP) or visceral muscle fluorescence (α-Tm, α-Mhc). Myotube leading edge F-actin levels were determined by normalizing mean fluorescence at the leading edge relative to internal fluorescence. Time-lapse microscopy was used to identify the position of the nascent myotubes prior to F-actin measurements (Fig. S7). Act57B.-593/+2.nlacZ fluorescence was measured in single nuclei and normalized to background fluorescence. Muscle size was determined by outlining individual DO2 muscles to obtain an area. All measurements were performed with Zen2011 software (Zeiss).

Cell culture and western blots

Schneider 2 (S2) cells were grown in Schneider's media supplemented with 10% FBS and Pen/Strep. Cells were passaged biweekly and split the day prior to transfection. On the day of the transfection, cells were seeded to a density of $1.0X10^6$ cells/mL in Schneider's media with FBS. 0.8mL of cells were transferred to one well of a 12-well plate. Transfections were performed with Effectene according to the manufacturer's instructions. 48hrs post-transfection, whole cell extracts were made by pelleting cells and resuspending in lysis buffer (20 mM Tris pH 7.5, 150 mM NaCl, 1% Triton-X, and protease inhibitors). Cells were lysed on ice for 10 minutes, followed by 10 min centrifugation. Western blots were performed as described (Mokalled et al., 2010) and imaged using the ChemiDoc XRS+ system (BioRad). A minimum of 3 blots was performed from independent transfections for each experiment shown.

Gateway technology was used to generate tagged Hoip constructs using the *hoip* cDNA clone (RE51843) as a PCR template.

Quantitative RT-PCR

Staged embryos were dechorionated and hand sorted to isolate homozygous mutants. RNA was extracted from embryos or S2 cells using TRizol, and cDNA was generated using Superscript III (Life Technologies). qPCR was performed with SYBR Select Master Mix using an ABI Prism 7000 (Life Technologies). Forward and reverse primers were designed to exons separated by at least one intron, except for splicing assay primers. Here, forward primers were designed to an exon and reverse primers were designed to the downstream intron (to detect unspliced transcripts) or to span the downstream splice donor/acceptor sites (to detect spliced transcripts). qPCR reactions were run in triplicate and normalized to *RpL32* or *GAPDH*. See Table S1 for primer sequences.

References

Baas, D., Caussanel-Boude, S., Guiraud, A., Calhabeu, F., Delaune, E., Pilot, F., Chopin, E., Machuca-Gayet, I., Vernay, A., Bertrand, S.*, et al.* (2012). CKIP-1 regulates mammalian and zebrafish myoblast fusion. J Cell Sci *125*, 3790-3800.

Bai, F., Groth, H.L., and Kawai, M. (2012). DCM-related tropomyosin mutants E40K/E54K over-inhibit the actomyosin interaction and lead to a decrease in the number of cycling cross-bridges. PLoS One *7*, e47471.

Berger, S., Schafer, G., Kesper, D.A., Holz, A., Eriksson, T., Palmer, R.H., Beck, L., Klambt, C., Renkawitz-Pohl, R., and Onel, S.F. (2008). WASP and SCAR have distinct roles in activating the Arp2/3 complex during myoblast fusion. J Cell Sci *121*, 1303-1313.

Bongiovanni, A., Romancino, D.P., Campos, Y., Paterniti, G., Qiu, X., Moshiach, S., Di Felice, V., Vergani, N., Ustek, D., and d'Azzo, A. (2012). Alix protein is substrate of Ozz-E3 ligase and modulates actin remodeling in skeletal muscle. J Biol Chem *287*, 12159-12171.

Buckingham, M., and Rigby, P.W. (2014). Gene regulatory networks and transcriptional mechanisms that control myogenesis. Dev Cell *28*, 225-238.

Bugyi, B., and Carlier, M.F. (2010). Control of actin filament treadmilling in cell motility. Annu Rev Biophys *39*, 449-470.

Buszczak, M., Paterno, S., Lighthouse, D., Bachman, J., Planck, J., Owen, S., Skora, A.D., Nystul, T.G., Ohlstein, B., Allen, A.*, et al.* (2007). The carnegie protein trap library: a versatile tool for Drosophila developmental studies. Genetics *175*, 1505-1531.

Chen, E.H., and Olson, E.N. (2004). Towards a molecular pathway for myoblast fusion in Drosophila. Trends Cell Biol *14*, 452-460.

Ciglar, L., and Furlong, E.E. (2009). Conservation and divergence in developmental networks: a view from Drosophila myogenesis. Curr Opin Cell Biol *21*, 754-760.

de Joussineau, C., Bataille, L., Jagla, T., and Jagla, K. (2012). Diversification of muscle types in Drosophila: upstream and downstream of identity genes. Curr Top Dev Biol *98*, 277-301.

Fisher, B., Weiszmann, R., Frise, E., Hammonds, A., Tomancak, P., Beaton, A., Berman, B., Quan, E., Shu, S., Lewis, S.*, et al.* (2012). BDGP insitu homepage.

Friedrich, B.M., Fischer-Friedrich, E., Gov, N.S., and Safran, S.A. (2012). Sarcomeric pattern formation by actin cluster coalescence. PLoS Comput Biol *8*, e1002544.

Gratz, S.J., Cummings, A.M., Nguyen, J.N., Hamm, D.C., Donohue, L.K., Harrison, M.M., Wildonger, J., and O'Connor-Giles, K.M. (2013). Genome engineering of Drosophila with the CRISPR RNA-guided Cas9 nuclease. Genetics *194*, 1029-1035.

Gross, S.R. (2013). Actin binding proteins: their ups and downs in metastatic life. Cell Adh Migr *7*, 199-213.

Gupton, S.L., Anderson, K.L., Kole, T.P., Fischer, R.S., Ponti, A., Hitchcock-DeGregori, S.E., Danuser, G., Fowler, V.M., Wirtz, D., Hanein, D.*, et al.* (2005). Cell migration without a lamellipodium: translation of actin dynamics into cell movement mediated by tropomyosin. J Cell Biol *168*, 619-631.

Johnson, A.N., Mokalled, M.H., Valera, J.M., Poss, K.D., and Olson, E.N. (2013). Post-transcriptional regulation of myotube elongation and myogenesis by Hoi Polloi. Development *140*, 3645-3656.

Karibe, A., Tobacman, L.S., Strand, J., Butters, C., Back, N., Bachinski, L.L., Arai, A.E., Ortiz, A., Roberts, R., Homsher, E.*, et al.* (2001). Hypertrophic cardiomyopathy caused by a novel alpha-tropomyosin mutation (V95A) is associated with mild cardiac phenotype, abnormal calcium binding to troponin, abnormal myosin cycling, and poor prognosis. Circulation *103*, 65-71.

Kawamura, K., Takano, K., Suetsugu, S., Kurisu, S., Yamazaki, D., Miki, H., Takenawa, T., and Endo, T. (2004). N-WASP and WAVE2 acting downstream of phosphatidylinositol 3-kinase are required for myogenic cell migration induced by hepatocyte growth factor. J Biol Chem *279*, 54862-54871.

Kelly, K.K., Meadows, S.M., and Cripps, R.M. (2002). Drosophila MEF2 is a direct regulator of Actin57B transcription in cardiac, skeletal, and visceral muscle lineages. Mech Dev *110*, 39-50.
Kiehart, D.P., and Feghali, R. (1986). Cytoplasmic myosin from Drosophila melanogaster. The Journal of cell biology *103*, 1517-1525.
Kim, J.H., Cho, A., Yin, H., Schafer, D.A., Mouneimne, G., Simpson, K.J., Nguyen, K.V., Brugge, J.S., and Montell, D.J. (2011). Psidin, a conserved protein that regulates protrusion dynamics and cell migration. Genes Dev *25*, 730-741.
Kim, J.H., Ren, Y., Ng, W.P., Li, S., Son, S., Kee, Y.S., Zhang, S., Zhang, G., Fletcher, D.A., Robinson, D.N.*, et al.* (2015). Mechanical tension drives cell membrane fusion. Dev Cell *32*, 561-573.
Kuhn, J.F., Tran, E.J., and Maxwell, E.S. (2002). Archaeal ribosomal protein L7 is a functional homolog of the eukaryotic 15.5kD/Snu13p snoRNP core protein. Nucleic Acids Res *30*, 931-941.
Liu, S., Li, P., Dybkov, O., Nottrott, S., Hartmuth, K., Luhrmann, R., Carlomagno, T., and Wahl, M.C. (2007). Binding of the human Prp31 Nop domain to a composite RNA-protein platform in U4 snRNP. Science *316*, 115-120.
Marttila, M., Lehtokari, V.L., Marston, S., Nyman, T.A., Barnerias, C., Beggs, A.H., Bertini, E., Ceyhan-Birsoy, O., Cintas, P., Gerard, M.*, et al.* (2014). Mutation update and genotype-phenotype correlations of novel and previously described mutations in TPM2 and TPM3 causing congenital myopathies. Hum Mutat *35*, 779-790.
Mokalled, M.H., Johnson, A., Kim, Y., Oh, J., and Olson, E.N. (2010). Myocardin-related transcription factors regulate the Cdk5/Pctaire1 kinase cascade to control neurite outgrowth, neuronal migration and brain development. Development *137*, 2365-2374.
Nose, A., Isshiki, T., and Takeichi, M. (1998). Regional specification of muscle progenitors in Drosophila: the role of the msh homeobox gene. Development *125*, 215-223.
Olson, T.M., Kishimoto, N.Y., Whitby, F.G., and Michels, V.V. (2001). Mutations that alter the surface charge of alpha-tropomyosin are associated with dilated cardiomyopathy. J Mol Cell Cardiol *33*, 723-732.
Ponti, A., Machacek, M., Gupton, S.L., Waterman-Storer, C.M., and Danuser, G. (2004). Two distinct actin networks drive the protrusion of migrating cells. Science *305*, 1782-1786.
Richardson, B.E., Beckett, K., Nowak, S.J., and Baylies, M.K. (2007). SCAR/WAVE and Arp2/3 are crucial for cytoskeletal remodeling at the site of myoblast fusion. Development *134*, 4357-4367.
Ridley, A.J., Schwartz, M.A., Burridge, K., Firtel, R.A., Ginsberg, M.H., Borisy, G., Parsons, J.T., and Horwitz, A.R. (2003). Cell migration: integrating signals from front to back. Science *302*, 1704-1709.
Rui, Y., Bai, J., and Perrimon, N. (2010). Sarcomere formation occurs by the assembly of multiple latent protein complexes. PLoS Genet *6*, e1001208.
Schejter, E.D., and Baylies, M.K. (2010). Born to run: creating the muscle fiber. Curr Opin Cell Biol *22*, 566-574.
Schnorrer, F., and Dickson, B.J. (2004). Muscle building; mechanisms of myotube guidance and attachment site selection. Dev Cell *7*, 9-20.
Schultz, A., Nottrott, S., Watkins, N.J., and Luhrmann, R. (2006). Protein-protein and protein-RNA contacts both contribute to the 15.5K-mediated assembly of the U4/U6 snRNP and the box C/D snoRNPs. Mol Cell Biol *26*, 5146-5154.

Figures

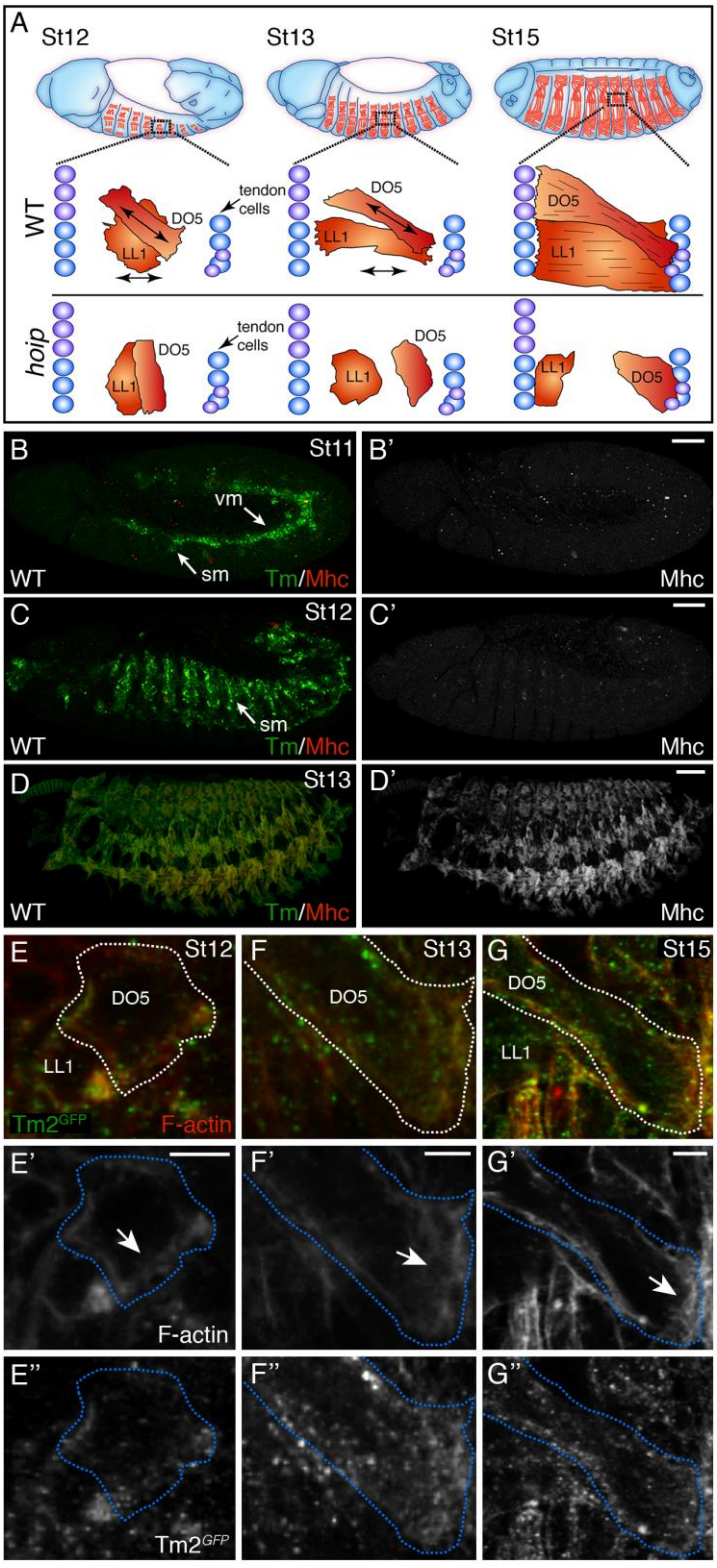

Figure 1. Tropomyosin expression and localization suggests a novel function. (A) Myotube elongation in *Drosophila* embryos. Bidirectional myotube elongation (double arrows) initiates during St12, continues through St13, and is largely complete by St15 when elongated muscles identify attachment sites associated with tendon cells. *hoip* embryos are defective in myotube elongation, in particular the Longitudinal Lateral 1 (LL1) and Dorsal Oblique 5 (DO5) muscles fail to elongate. (B-D) WT embryos labeled for Tropomyosin (Tm, green) and Mhc (red). Tm is first detected in the somatic muscle (SM) founder cells during St11 (B). Tm is robustly expressed in SM during myotube elongation (St12, C) while SM Mhc is largely undetectable until St13 (D). (B'-D') Mhc expression. (E-G) *Tm2*^{GFP} protein-trap embryos double labeled for GFP (green) and F-actin (phalloidin, red). Tm2^{GFP} co-localized with F-actin at the myotube leading edge (white arrows). (E'-G') F-actin. (E''-G'') Tm2^{GFP}. (VM) visceral muscle. Scale bars represent 50μm (B-D) and 5μm (E-G). Embryos are oriented with anterior to the left and dorsal to the top in this and subsequent figures.

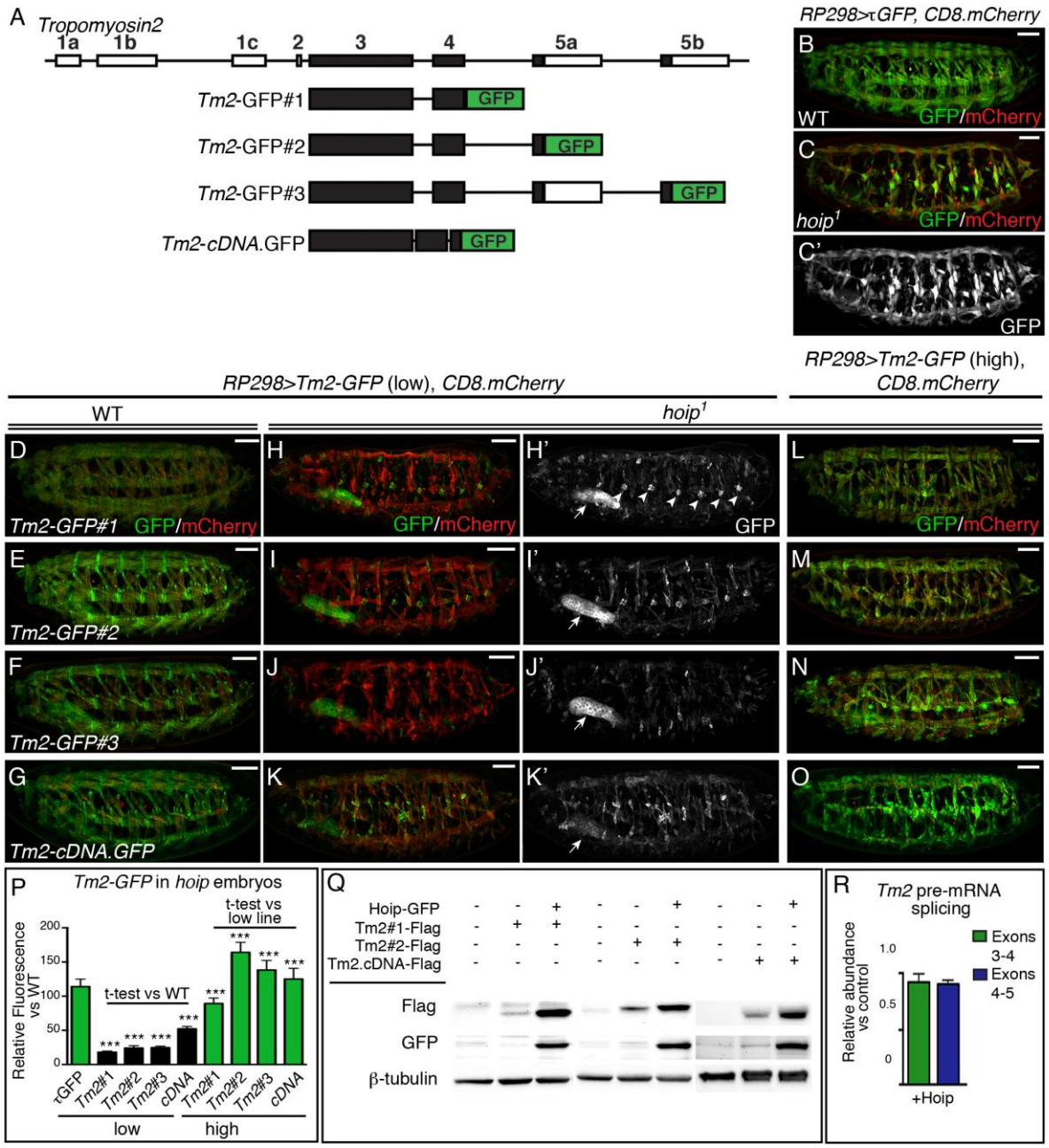

Figure 2. Hoip directs Tm2 protein expression but not *Tm2* pre-mRNA splicing. (A) Diagram of the *Tm2* locus and the *Tm2-GFP* constructs. Boxes represent exons; shaded regions denote the coding region. *Tm2* encodes two alternative final exons (5a/b). Both low-level and high-level expressing insertions were recovered for each construct. (B-O) Live St16 embryos. The somatic muscle driver *RP298.gal4* was used to co-express *CD8.mCherry* and *τGFP* (B,C) or *Tm2-GFPs* (D-O). (B,C) τGFP and CD8.mCherry were expressed at comparable levels in WT and *hoip*^{1} embryos. (C') τGFP. Low-level expressing

Tm2-GFP#1-3 and *Tm2-cDNA.GFP* produced Tm2-GFP in WT embryos (D-G), but Tm2-GFP was largely undetectable in *hoip*^{1} embryos (H-K). *RP298.gal4* also directs transgene expression in the salivary gland (arrows) and the PNS (arrowheads). Non-muscle tissues showed robust Tm2-GFP in *hoip*^{1} embryos. (H'-K') Tm2-GFP expression. (L-O) Tm2-GFP from high-level expressing *Tm2-GFP* constructs was detectable in *hoip*^{1} embryos. (P) Quantification of GFP fluorescence in *hoip*^{1} DO2 muscles relative to WT. DO2 muscles elongate in *hoip*^{1} embryos and were used to assay transgene expression in this and subsequent figures. (***) $p<0.001$. (Q) Western blots from S2 cells co-transfected with Hoip.GFP and the *Tm2* constructs shown in (A) with a C-terminal Flag tag. Hoip promoted Tm2 protein expression from both cDNA and genomic constructs. (R) *Tm2-#2* splicing in S2 cells transfected with Hoip or control vector. qPCR results show the abundance of intron-free transcripts compared to intron-containing transcripts relative to control transfected cells. Scale bars represent 50μm. Error bars represent SEM.

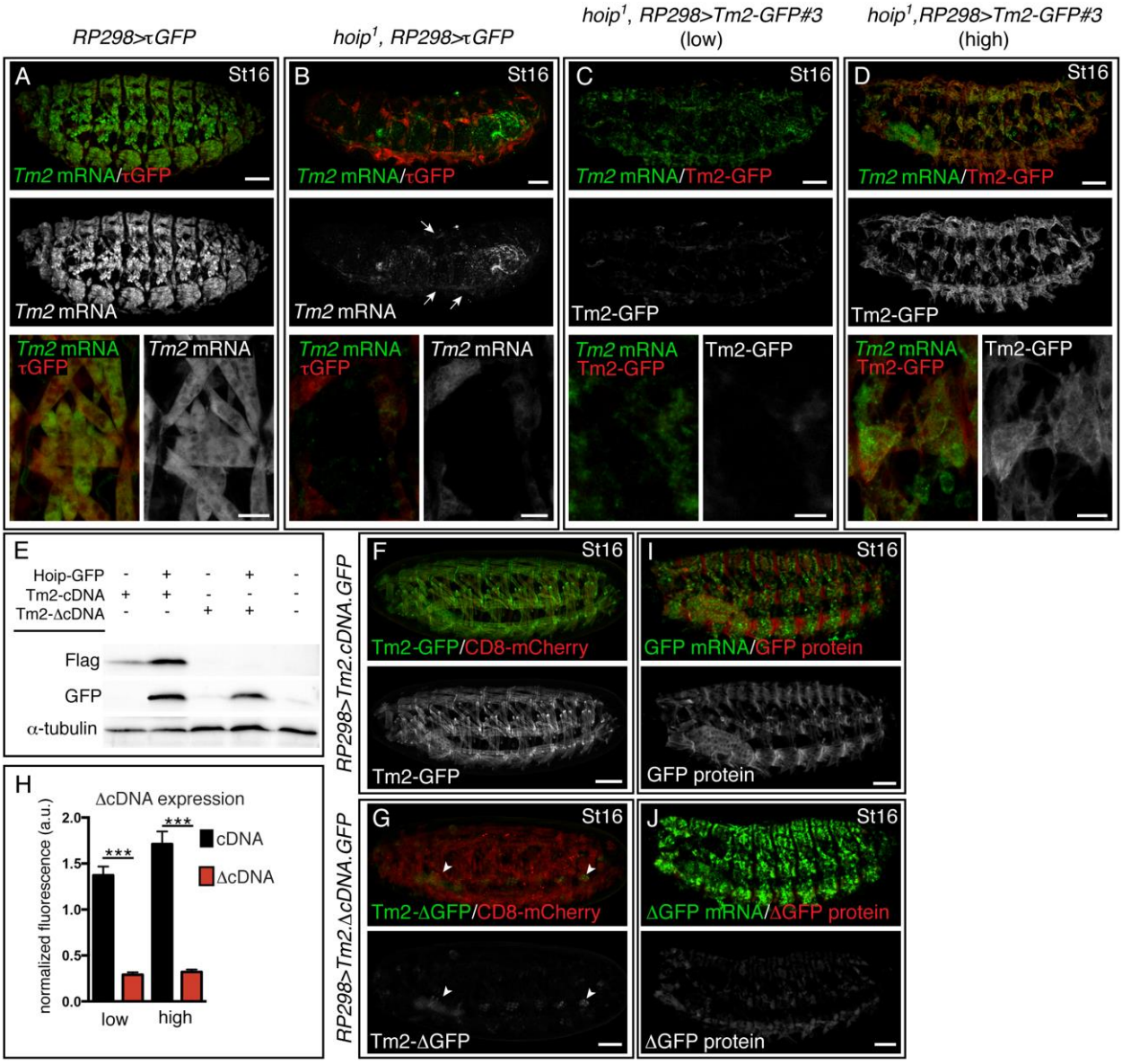

Figure 3. *Tm2* coding region sequences direct somatic muscle protein expression. (A-D) St16 embryos that expressed *τGFP* (A,B) or *Tm2-GFP#3* (C,D) under the control of *RP298.gal4* double labeled for *Tm2* mRNA (green) and GFP (red). WT embryos expressed *Tm2* in all SMs (A), whereas *hoip*^{1} embryos expressed only weak *Tm2* in only the dorsal and ventral muscles (B, arrows). (C) *hoip*^{1} embryos that expressed low-level *Tm2-GFP#3* accumulated *Tm2* RNA in the cytoplasm but did not express significant Tm2-GFP protein. (D) *hoip*^{1} embryos that expressed high-level *Tm2-GFP#3* expressed more Tm2-GFP protein than low-level expressing *Tm2-GFP#3* embryos. (E) S2 cells transfected with Hoip and the Tm2-ΔcDNA construct, that lacks the first 260bp downstream of the start codon, produced

less Tm2 protein than cells transfected with the full-length construct. (F,G) Live St16 embryos that co-expressed *CD8.mCherry* and *Tm2-cDNA.GFPs* under the control of *RP298.gal4*. Tm2-ΔGFP protein is expressed in non-muscle tissues (arrowheads) but not SM. (H) Normalized Tm2-GFP expression in DO2 muscles. (***) $p<0.001$. (I,J) St16 embryos that expressed *Tm2-cDNA.GFPs* under the control of *RP298.gal4* double labeled for *GFP* mRNA (green) and GFP protein (red). *Tm2-cDNA.GFP* and *Tm2-ΔcDNA.GFP* RNAs accumulated at equal levels in the cytoplasm, but only the full-length Tm2-GFP protein was expressed at high levels in SM. Scale bars represent 10μm (A-D) and 50μm (F-J). Error bars represent SEM. (SM) somatic muscle.

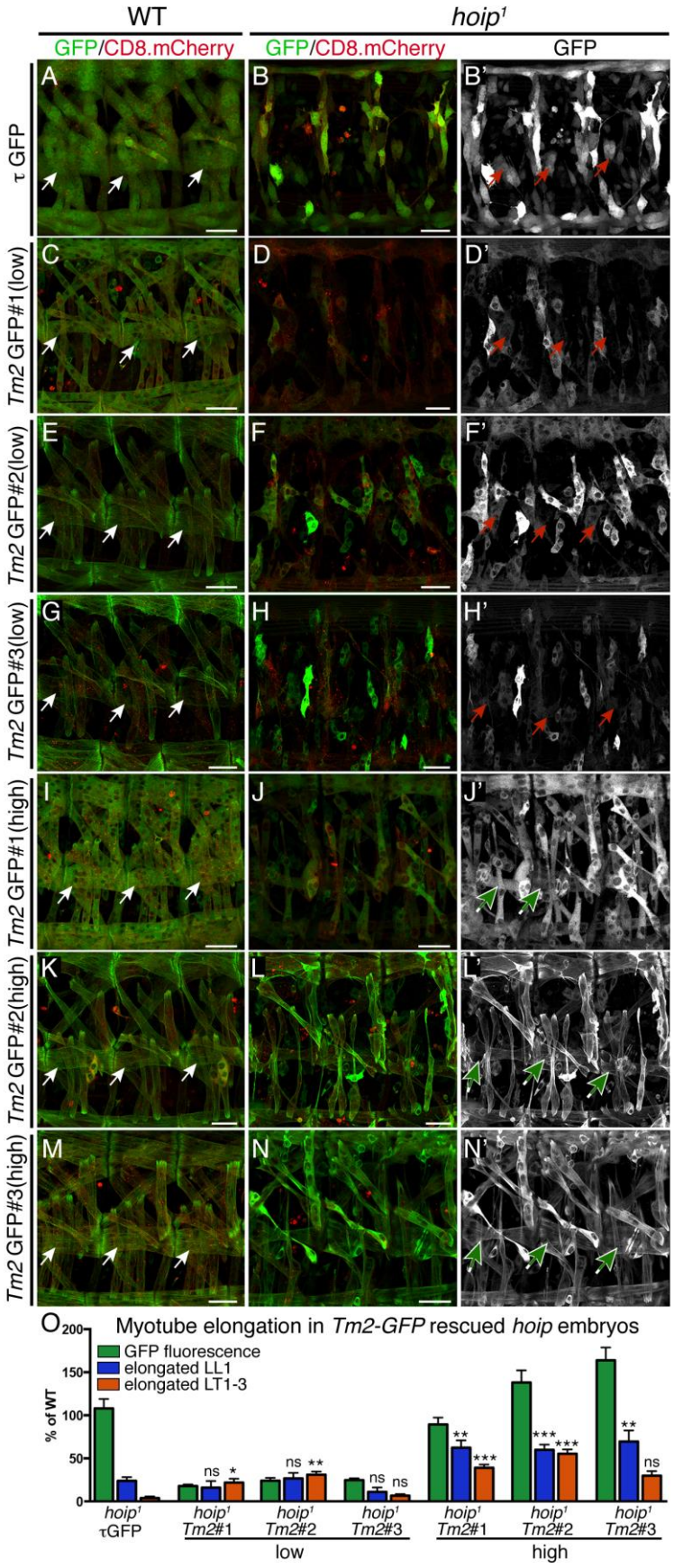

Figure 4. *Tm2* rescues myotube elongation defects in *hoip*^{1} embryos. Live St16 embryos that co-expressed *CD8.mCherry* and *τ.GFP* (A,B), low-level *Tm2-GFPs* (C-H), or high-level *Tm2-GFPs* (I-N) under the control of *RP298.gal4*. White arrows denote properly elongated LL1 muscles in WT embryos. (A,B) *τ.GFP* and *CD8.mCherry* were expressed at comparable levels in WT and *hoip*^{1} embryos. LL1 muscles failed to elongate (red arrows) in *hoip*^{1} embryos that expressed *τ.GFP*. (C-H) Compared to WT embryos, *hoip*^{1} embryos showed reduced Tm2-GFP fluorescence from low-level expressing lines. A majority of LL1 muscles failed to elongate in *hoip*^{1} embryos that expressed low-level *Tm2-GFPs*. (I-N) Tm2-GFP fluorescence from high-level expressing lines was comparable between WT and *hoip*^{1} embryos. LL1 muscles showed improved elongation and morphology in *hoip*^{1} embryos that expressed high-level *Tm2-GFPs* (green arrows). LT1-3, DO3-4, and LO1 muscles also elongated in the presence of Tm2-GFP. mCherry was used to assess elongation is muscles that did not express Tm2-GFP. (B'-N') GFP expression. (O) Quantification of GFP fluorescence and muscle morphology in *hoip*^{1} embryos that expressed GFP transgenes. Significance was determined between *hoip*^{1}, *τ.GFP* embryos and *hoip*^{1}, *Tm2-GFP* embryos. (*) $p<0.05$, (**) $p<0.01$, (***) $p<0.001$, (ns) not significant. Scale bars represent 20μm. Error bars represent SEM.

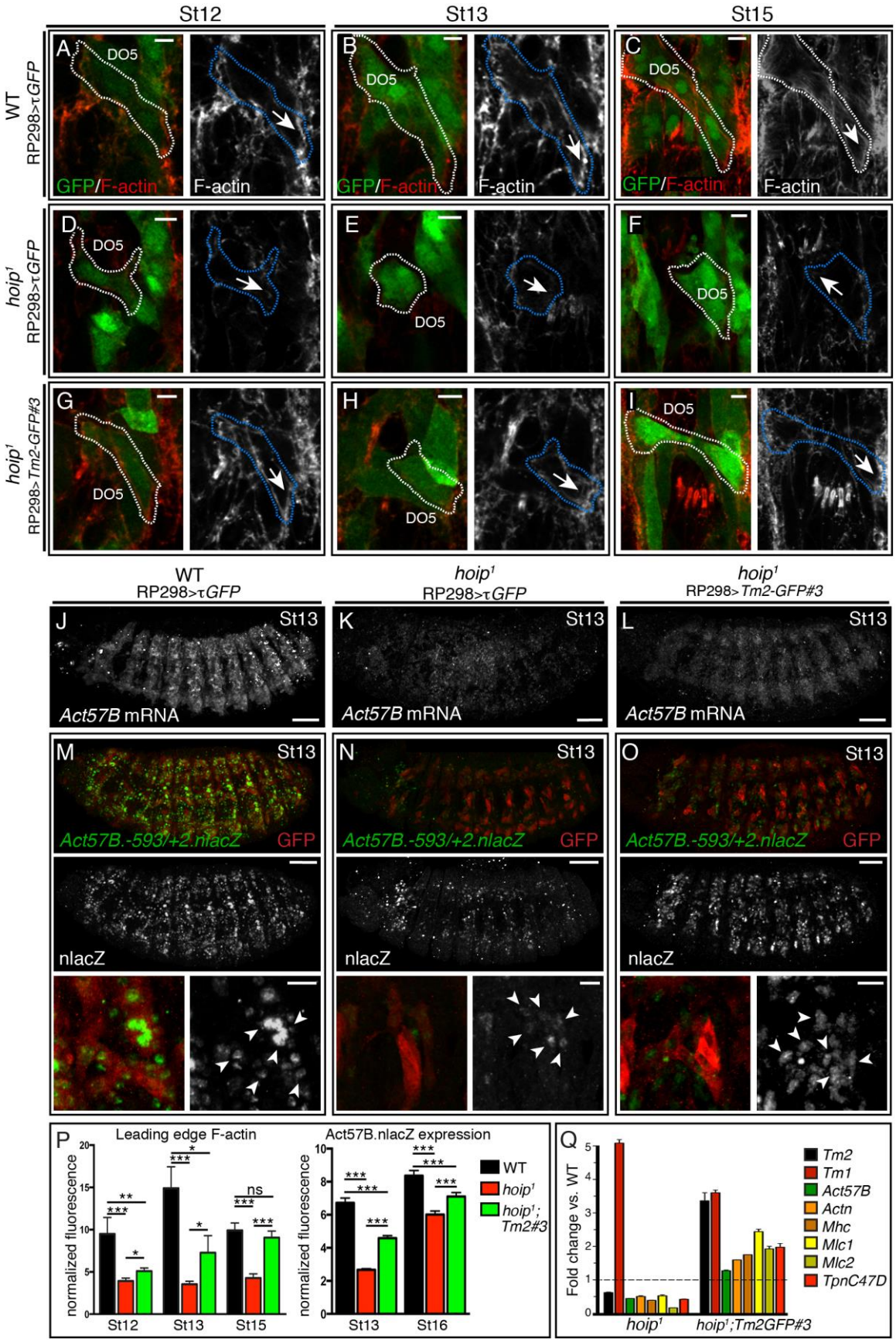

Figure 5. *Tm2* restores actin expression in *hoip[1]* embryos. (A-I) Embryos that expressed *τGFP* (A-F) or one copy of *Tm2-GFP#3* (G-I) under the control of *RP298.gal4* co-labeled for F-actin (phalloidin, red). (A-C) WT embryos showed robust F-actin accumulation at the leading edge of elongating myotubes (St12-13; A,B) and during target site recognition (St15; C). The DO5 muscle is outlined in white or blue throughout the figure. Arrows denote one leading-edge. (D-F) *hoip[1]* embryos showed reduced F-actin accumulation at DO5 myotube leading edges throughout myogenesis. (G-I) *hoip[1]* embryos that expressed high-level *Tm2-GFP#3* showed improved F-actin accumulation at myotube leading edges compared to control *hoip[1]* embryos. (J-L) St13 embryos that expressed *τ.GFP* (J,K) or one copy of *Tm2-GFP#3* (L) labeled for *Act57B* mRNA. *hoip[1]* embryos showed reduced *Act57B. hoip[1]* embryos that expressed *Tm2-GFP#3* showed improved *Act57B* expression. (M-O) St13 *Act57B.-593/+2.nlacZ* embryos that expressed *τ.GFP* (M,N) or one copy of *Tm2-GFP#3* (O). *hoip[1]* embryos showed reduced lacZ expression. *hoip[1]* embryos that expressed *Tm2-GFP#3* showed improved lacZ expression. Arrowheads show a subset of somatic muscle nuclei. (P) Quantification of leading-edge F-actin and *Act57B.-593/+2.nlacZ* expression. (Q) qPCR of mRNA isolated from St17 embryos. Sarcomeric transcripts are downregulated in *hoip[1]* embryos and largely restored in *hoip[1]* embryos that expressed *Tm2-GFP#3*. The enrichment of *Tm1* in *hoip[1]* embryos suggests a compensatory mechanism may regulate Tropomyosin levels. (*) $p<0.05$, (**) $p<0.01$, (***) $p<0.001$. Scale bars represent 5μm (A-I) and 50μm or 10μm (J-O). Error bars represent SEM.

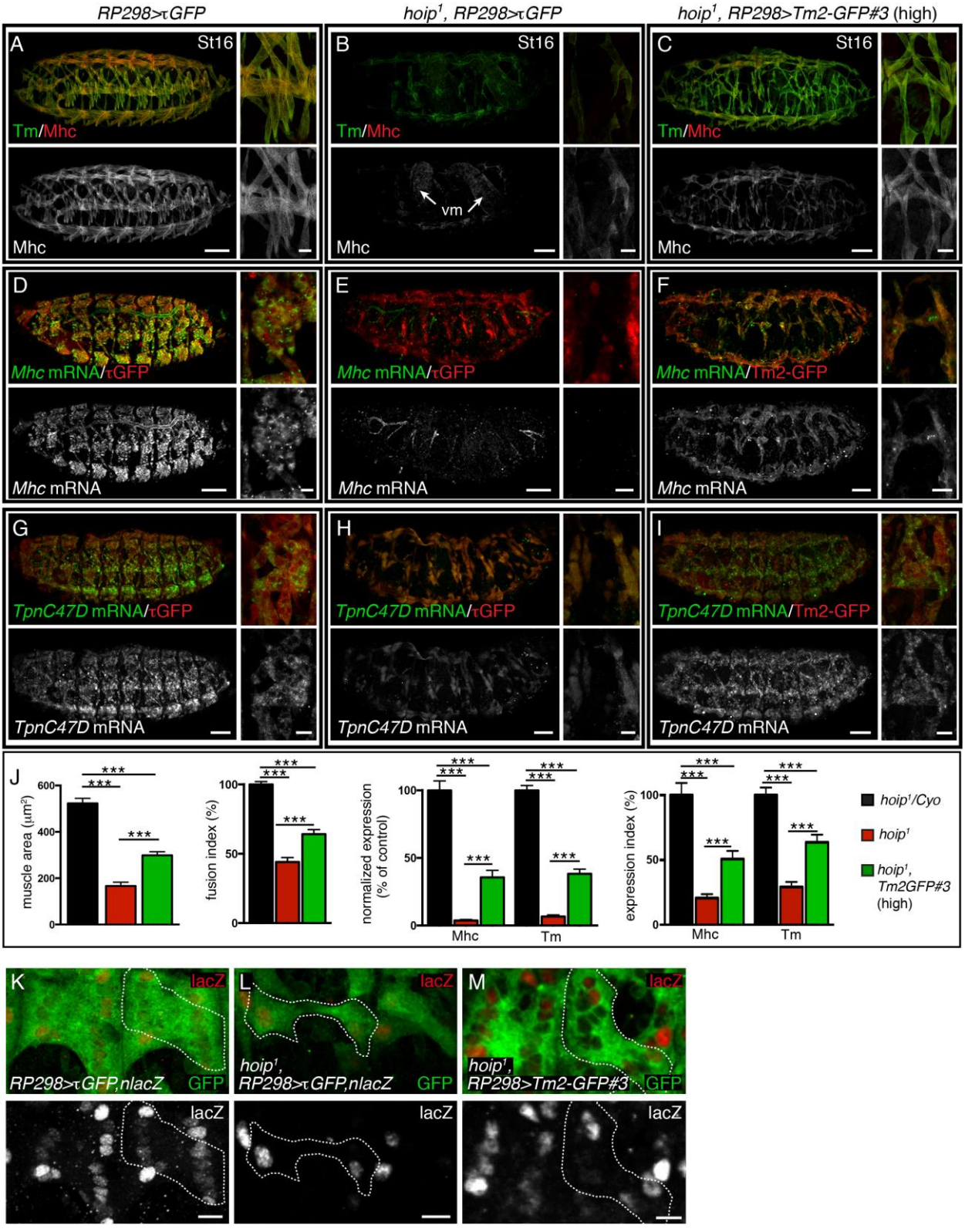

Figure 6. *Tm2* restores sarcomeric gene expression and promotes myoblast fusion in *hoip¹* embryos. (A-I) St16 embryos that expressed *τGFP* or one copy of *Tm2-GFP#3* under the control of *RP298.gal4* co-labeled for (A-C) Tropomyosin (Tm, green) and Mhc (red), (D-

F) *Mhc* mRNA (green) and GFP (red), or (G-I) *TpnC47D* mRNA (green) and GFP (red). Tm and Mhc protein expression is dramatically reduced in *hoip*^{1} embryos (A,B). *Tm2-GFP#3* partially restored Mhc protein expression *hoip*^{1} embryos (C). *Mhc* and *TpnC47D* mRNAs were also reduced in *hoip*^{1} embryos (D,E,G,H), and restored in *hoip*^{1} embryos that expressed *Tm2-GFP#3* (F,I). (J) Quantification of DO2 muscle size, myoblast fusion, and Mhc and Tm protein expression in St16 embryos. The fusion index represents the percentage of RP298.nlacZ positive nuclei (per hemisegment) versus control embryos. The expression index represents protein expression normalized to muscle area versus control embryos. (K-M) DO2 muscles from embryos that co-expressed RP298.lacZ and either *τGFP* or one copy of *Tm2-GFP#3* under the control of *RP298.gal4. hoip*^{1} DO2 muscles had fewer nuclei compared to WT, but did elongate. *Tm2-GFP#3* increased the number of nuclei in *hoip*^{1} DO2 muscles. (*) $p<0.05$, (**) $p<0.01$, (***) $p<0.001$. Scale bars represent 50μm (low magnification) and 10μm (high magnification). Error bars represent SEM.

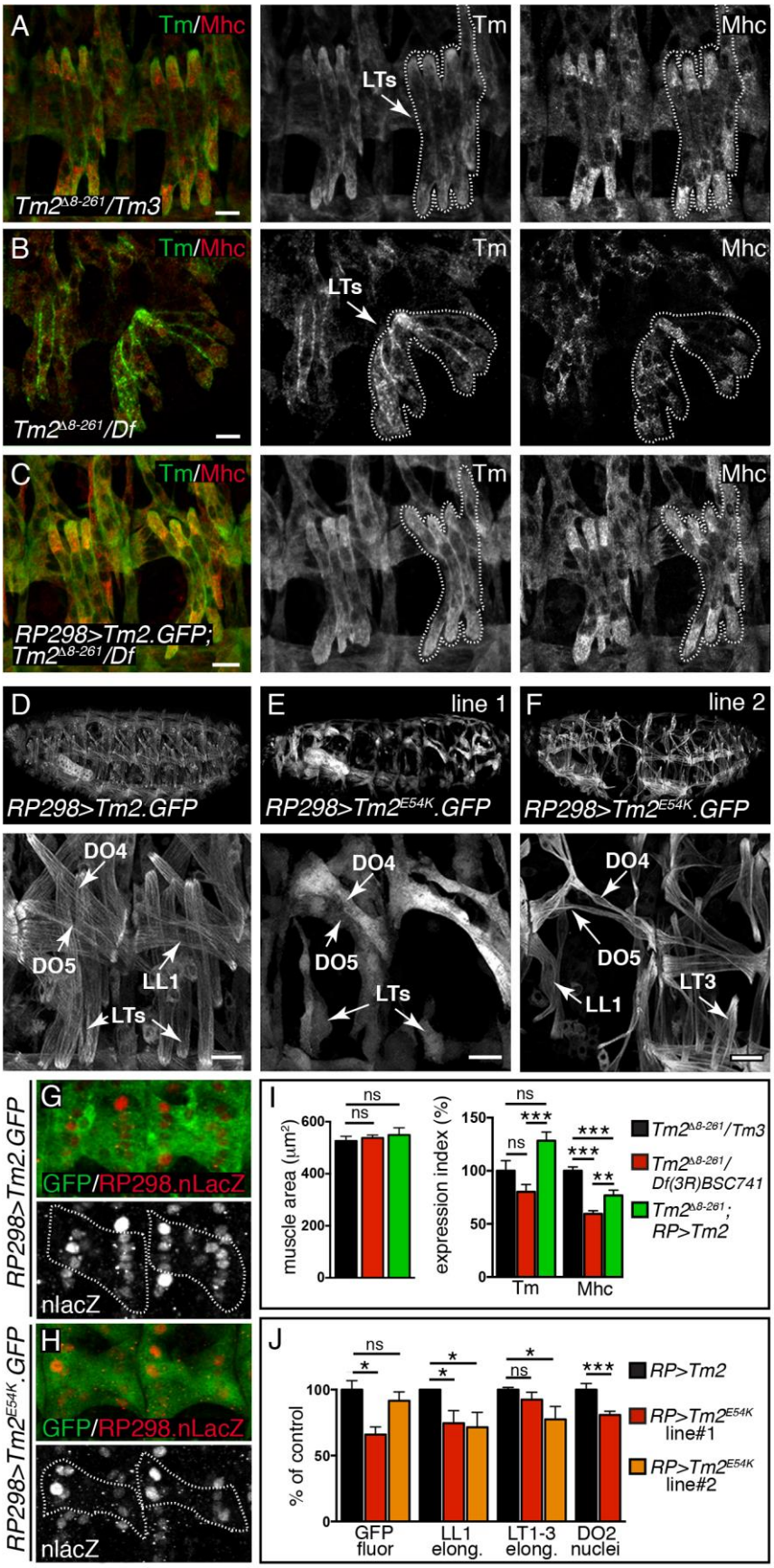

Figure 7. Tm2 regulates Mhc expression and directs myotube elongation. (A-C) St16 embryos labeled for Tropomyosin (Tm, green) and Mhc (red). (A,B) *$Tm2^{\Delta 8\text{-}261}$/Df(3R)BSC741* embryos expressed significant Tropomyosin protein, but showed reduced Mhc protein expression compared to control embryos. *$Tm2^{\Delta 8\text{-}261}$/Df(3R)BSC741* embryos also showed elongation defects at a low frequency (LT muscles from two segments are outlined). (C) Tm2.GFP restored Mhc protein expression in *$Tm2^{\Delta 8\text{-}261}$* embryos. (D-F) Live St17 embryos that expressed *Tm2-cDNA.GFP* or *$Tm2^{E54K}$-cDNA.GFP* under the control of *RP298.gal4*. LL1 and LT somatic muscles that expressed *$Tm2^{E54K}$* showed elongation defects. *$Tm2^{E54K}$* also disrupted DO5 muscle morphology (notice the bifurcated DO5 in F). (G,H) DO2 muscles from St16 RP298.nlacZ embryos that co-expressed *Tm2-cDNA.GFP* or *$Tm2^{E54K}$-cDNA.GFP*. The number of DO2 nuclei is reduced in embryos that expressed *$Tm2^{E54K}$-cDNA.GFP*. (I) DO2 muscle size and Mhc/Tm expression indexes. (J) Quantification of *$Tm2^{E54K}$-cDNA.GFP* expression, myotube elongation, and DO2 nuclei relative to *Tm2-cDNA.GFP*. Scale bars represent 10μm. (*) $p<0.05$, (**) $p<0.01$, (***) $p<0.001$. Error bars represent SEM. See Fig. S1 for muscle abbreviations.

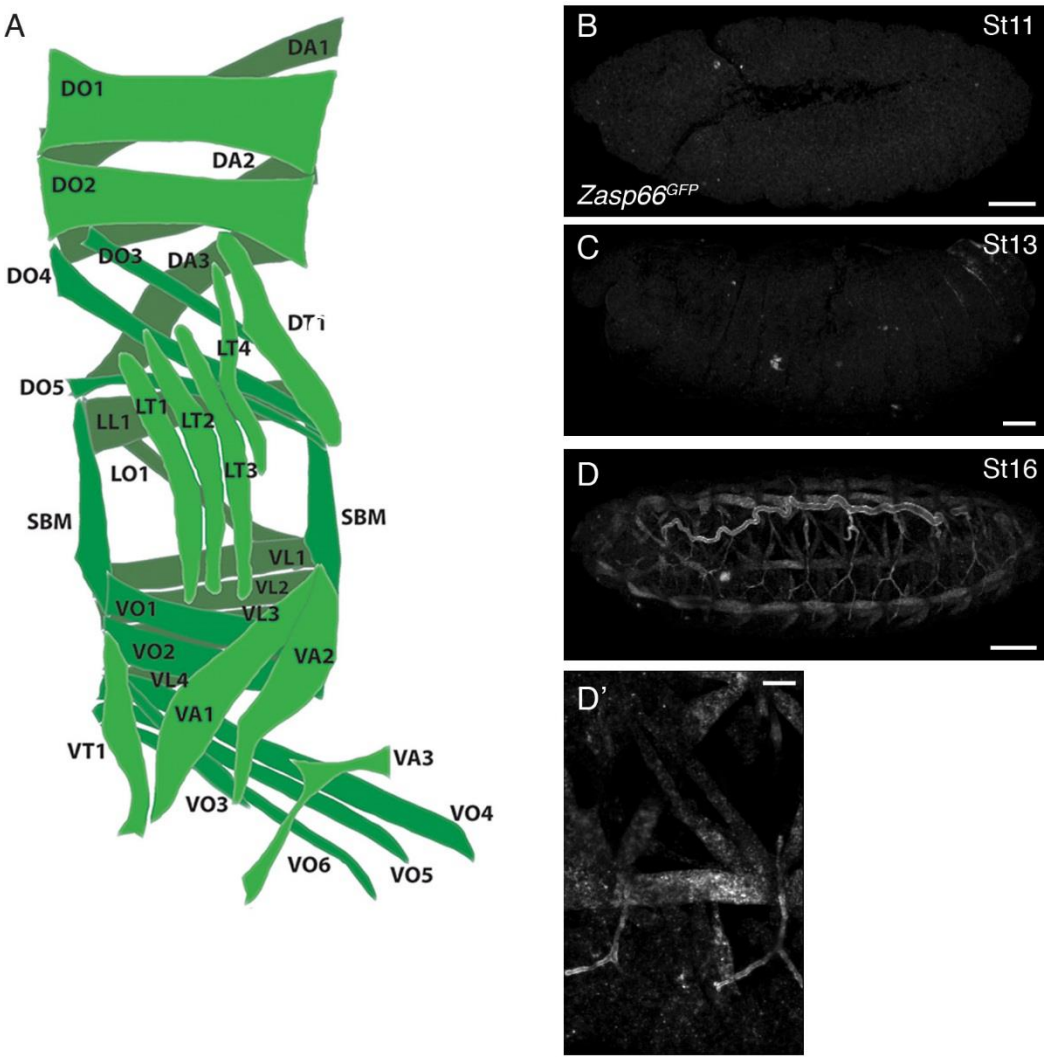

Figure S1. Zasp66 expression initiates late in myogenesis. (A) Somatic muscle diagram for one embryonic segment. Adapted from (Ruiz-Gomez et al., 1997). (B-D) *Zasp66*^{GFP} (protein trap) embryos labeled with α-GFP. Robust GFP expression is not detected until St16. Scale bars represent 50μm (B-D) and 10μm (D').

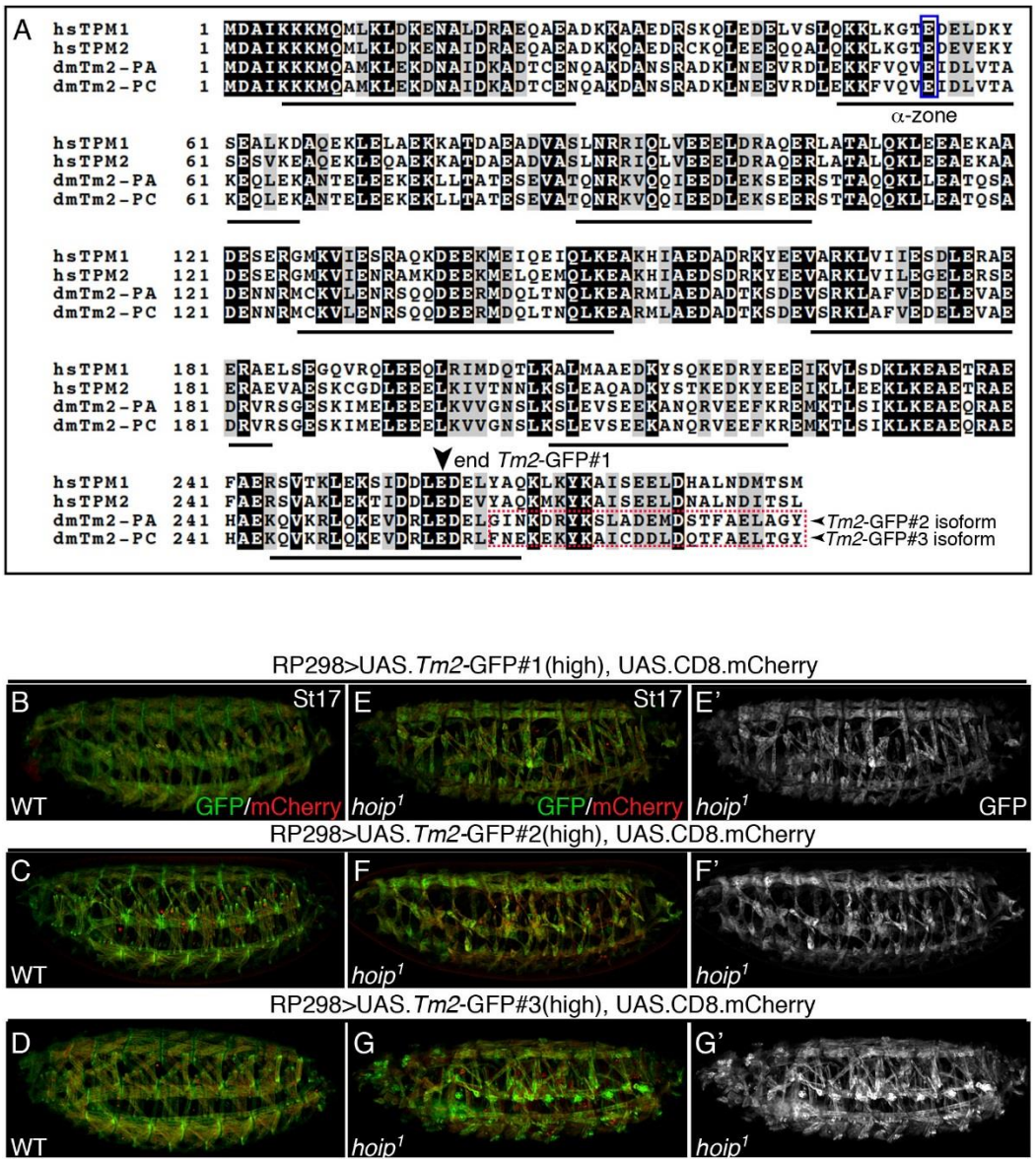

Figure S2. High-level *Tm2-GFPs* direct Tm2-GFP protein expression in *hoip*^{1} embryos. (A) Protein alignment of human TPM1 and TPM2 with two isoforms of *Drosophila* Tm2 (dmTm2). *Tm2* encodes two alternative final exons (5a/b). Isoform PC contains exon 5a; isoform PA contains exon 5b. The C-termini of the Tm2-GFPs are noted. Tropomyosin is a coiled coil protein comprised of 7 pseudo repeat domains, each of which contains an α-zone (underlined, adapted from Marttila et al., 2014). The E54K mutation is conserved and falls within the second α-zone. (B-G) Live St16 embryos. The somatic muscle driver *RP298.gal4* was used to co-express *CD8.mCherry* and high-level *Tm2-GFPs*. GFP fluorescence is comparable between WT (B-D) and *hoip*^{1} embryos (E-G). (E'-G') GFP.

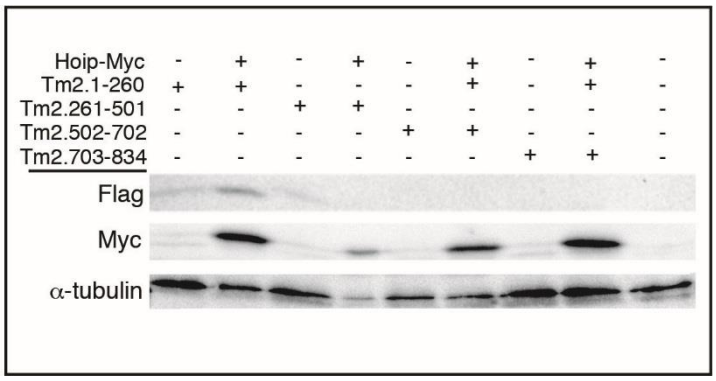

Figure S3. Mapping Hoip-responsive sequences in the *Tm2* coding region. Western blots from S2 cells transfected with Hoip.Myc and a series of *Tm2* coding region fragments. All *Tm2* constructs have a start codon in frame with a C-terminal Flag tag. The base pairs from the *Tm2* coding region used to generate each construct are given. Only the first 260bp of *Tm2* are Hoip responsive.

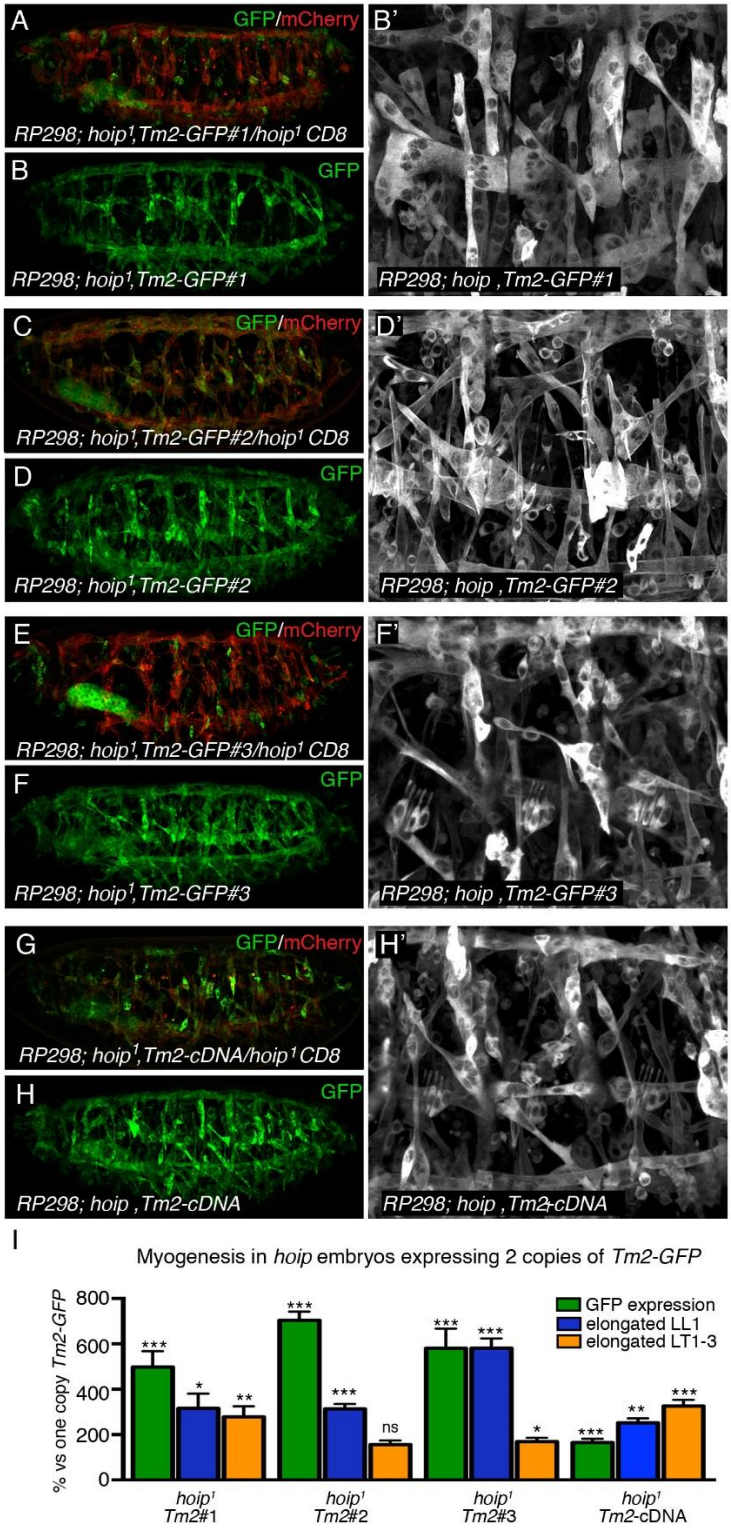

Figure S4. Rescue of the *hoip*^{1} myotube elongation phenotype by Tm2. (A-H) Live St16 embryos. *RP298.gal4* was used to express low-level *Tm2-GFPs* from a single copy of each transgene (A,C,E,G) or from two copies of each transgene (B,D,F,H) in *hoip*^{1} embryos. Single

copy embryos co-expressed CD8.mCherry to normalize Gal4 availability. *hoip*^{1} embryos that expressed *Tm2-GFPs* from a single copy showed reduced GFP expression compared to *hoip*^{1} embryos that expressed *Tm2-GFPs* from two copies. In addition, two copy embryos showed improved myotube elongation. (B',D',F',H') High magnification views of the embryos shown in (B,D,F,H). (I) Quantification of GFP fluorescence (DO2) and muscle morphology in *hoip*^{1} embryos that expressed *Tm2-GFP* transgenes. Significance was determined between *hoip*^{1} embryos that expressed one copy of the low-level *Tm2-GFPs* versus *hoip*^{1} embryos that expressed two copies. (*) $p<0.05$, (**) $p<0.01$, (***) $p<0.001$. Error bars represent SEM.

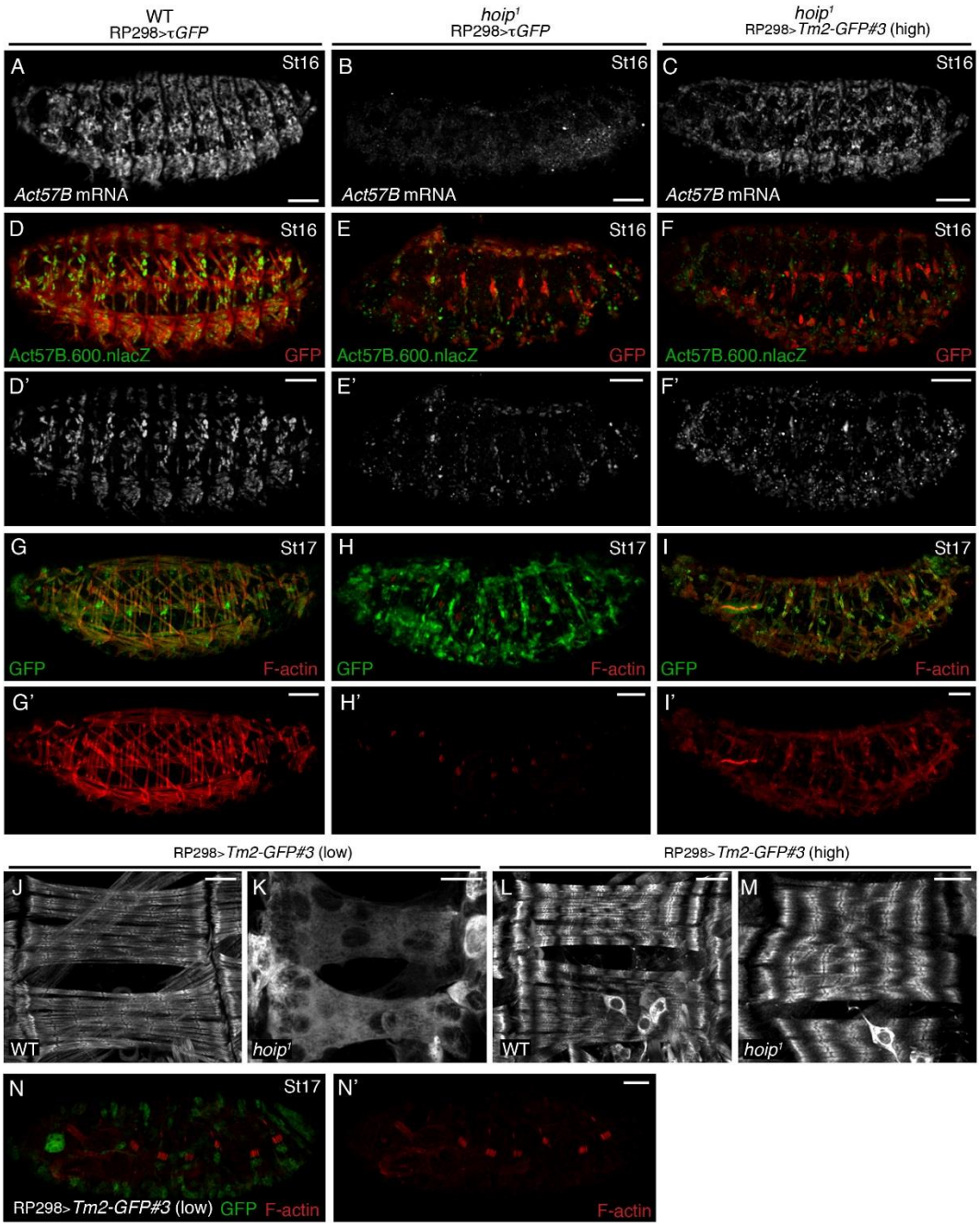

Figure S5. *Tm2* restores *Act57B* expression, F-actin assembly, and sarcomerogenesis in *hoip*^{1} embryos. (A-C) St16 embryos that expressed *τ.GFP* (A,B) or one copy of *Tm2-GFP#3* (C) labeled for *Act57B* mRNA. *hoip*^{1} embryos showed reduced SM *Act57B. hoip*^{1} embryos that expressed *Tm2-GFP#3* showed improved *Act57B* expression. (D-F) St16 *Act57B.600.nlacZ* embryos that expressed *τ.GFP* (D,E) or one copy of *Tm2-GFP#3* (F). *hoip*^{1} embryos showed

reduced lacZ expression. *hoip*^{1} embryos that expressed *Tm2-GFP#3* showed improved lacZ expression. (G-I, N) St17 embryos that expressed *τ.GFP* (G,H) or one copy of *Tm2-GFP#3* (I) under the control of *RP298.gal4* co-labeled for F-actin (phalloidin, red). (G) WT embryos showed robust F-actin in myofibrils. (H) F-actin was absent from the SM of *hoip*^{1} embryos. F-actin is detectable in the VM and unknown structures in the ectoderm. (I) *hoip*^{1} embryos that expressed high-level *Tm2-GFP#3* showed improved F-actin accumulation in the SM compared to *hoip*^{1} embryos. (J,K) DO1 and DO2 muscles from St17 embryos that expressed low-level *Tm2-GFP#3*. Low-level Tm2-GFP#3 incorporated into sarcomeres in WT but not *hoip*^{1} embryos. Confocal laser levels were increased between (J) and (K) to detect Tm2-GFP#3. (L,M) DO1 and DO2 muscles from St17 embryos that expressed high-level *Tm2-GFP#3*. High-level Tm2-GFP#3 incorporated into sarcomeres in both WT and *hoip*^{1} embryos. (N) *hoip*^{1} embryos that expressed low-level *Tm2-GFP#3* showed SM F-actin levels that were comparable to *hoip*^{1} embryos. (SM) somatic muscle, (VM) visceral muscle

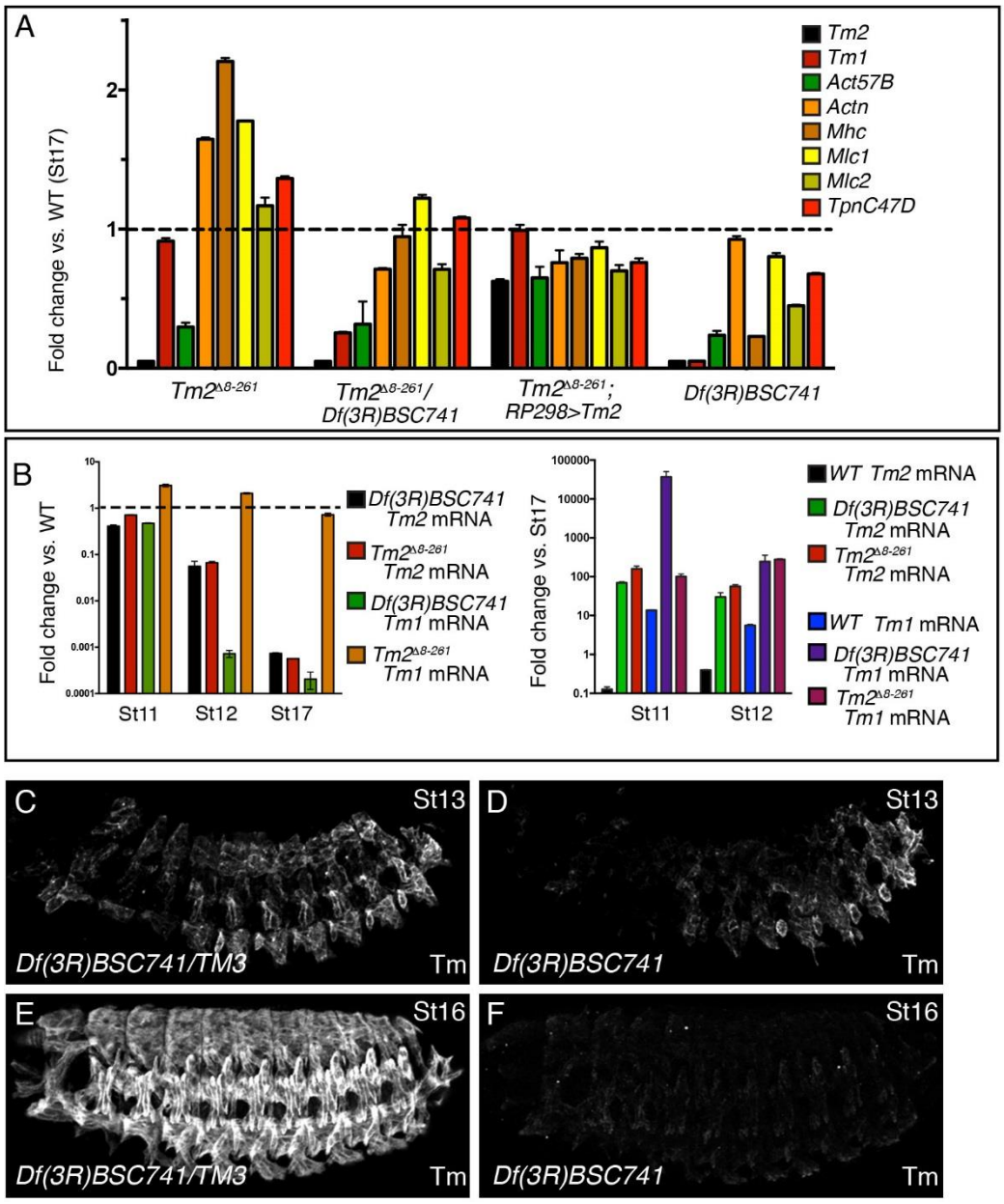

Figure S6. Maternally contributed *Tm1* and *Tm2* mRNAs promote Tropomyosin expression through St16. (A) qPCR of mRNA isolated from St17 embryos. *Tm2*$^{\Delta 8\text{-}261}$ is a genomic deletion that begins in the first coding exon and extends past the final coding exon. *Df(3R)BSC741* deletes *Tm1*, *Tm2,* and nineteen additional genes. *Tm2*$^{\Delta 8\text{-}261}$*/Df(3R)BSC741* transheterozygous embryos showed reduced *Act57B* abundance, which was partially rescued in mutant embryos that expressed *Tm2.GFP* under the control of *RP298.gal4.* (B) *Tm2* mRNA is detectable in *Tm2*$^{\Delta 8\text{-}261}$ and *Df(3R)BSC741* homozygous embryos at St11 and St12, but not St17. *Tm1* mRNA is enriched in St11-12 *Tm2*$^{\Delta 8\text{-}261}$ embryos suggesting *Tm1* can compensate for *Tm2*. (C-F) Embryos labeled with α-Tropomyosin (Tm). *Df(3R)BSC741* embryos expressed significant Tm protein at St13 (C,D), and Tm could still be detected in somatic muscle at St16.

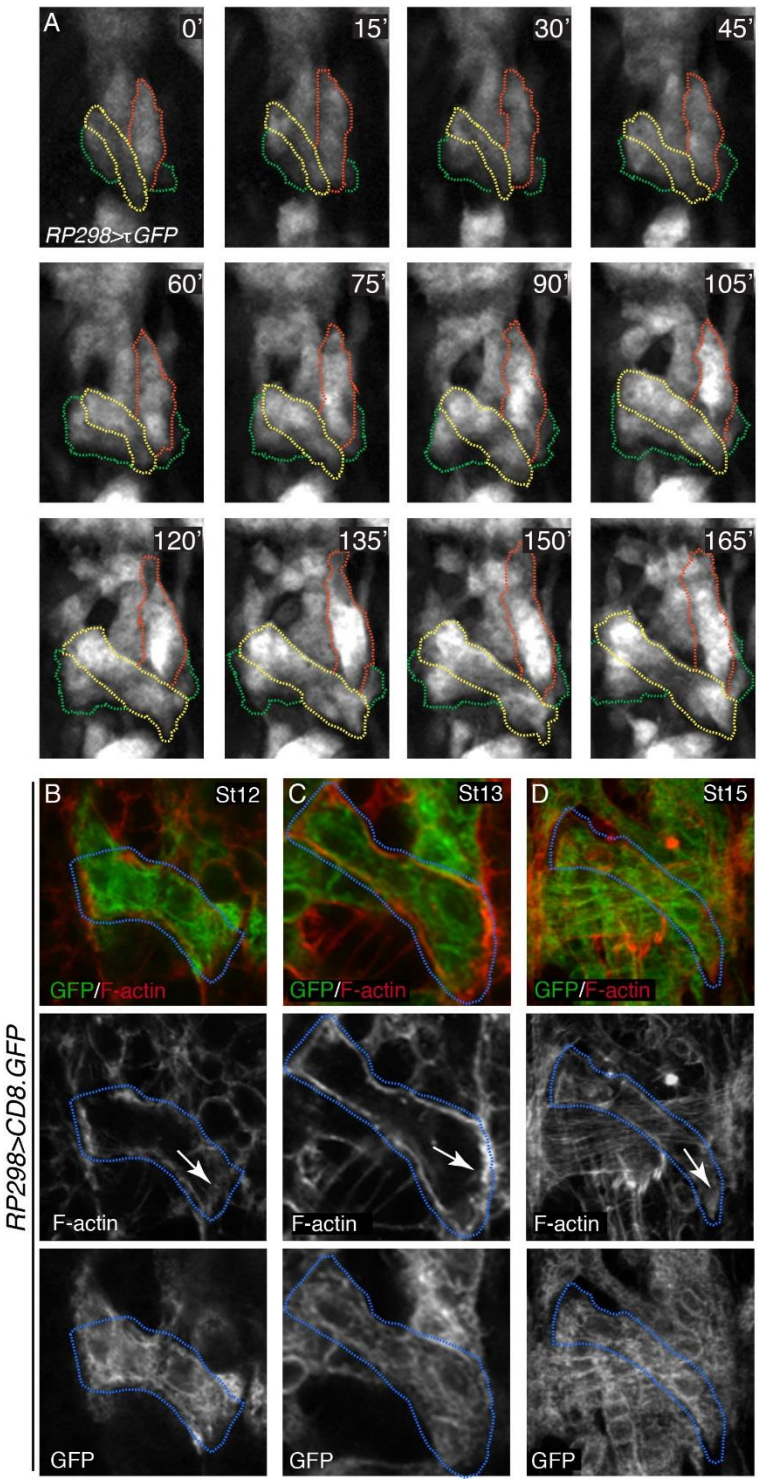

Figure S7. Time lapse microscopy. (A) Live myotube elongation in a single embryonic segment. *RP298.gal4* was used to express *τGFP*. Muscles shown include LL1 (green), DO5 (yellow), and DT1 (orange). (B-D) St12-15 embryos that expressed *CD8.GFP* under the control of *RP298.gal4* double labeled for GFP (green) and phalloidin (red). The DO5 muscle is outlined. Leading edge F-actin (arrows) corresponds with the boundary of CD8/membrane expression.

Table S1. Primers for qPCR

Primer Name	Sequence
TM2 F	5'-CAG CTG ACC AAC CAG TTG AA-3'
TM2 R	5'-GAC ACC TCC AGG GAC TTC AG-3'
TM1 F	5'-CAA GCG ATG AAA GTC GAC AA-3'
TM1 R	5'-CGG TCT GGA TCT TCT TCT GC-3'
Act57B F	5'-GCC TAG CAC CAA CAC TAG CA-3'
Act57B R	5'-CGC GAG CGA TTA ACA AGT GG-3'
Actn F	5'-CAA CGA GCT GAA GGC CCT AA-3'
Actn R	5'-CTT CTC CAG GAT TCG CTC GG-3'
Mhc F	5'-GTG CCG GAA AGA CTG AGA AC-3'
Mhc R	5'-GCA CCA GCC AGT TTA CCA GT- 3'
Mlc1 F	5'-CAA CTT CAC GCT TTG GAA CA-3'
Mlc1 R	5'-AGC TCA TCC GCG ATA CAG TT-3'
Mlc2 F	5'-ACC ACC CTC TTC CTT GGT CT-3'
Mlc2 F	5'-CAG CCA GAG ATT CAG TGT GC-3'
TpnC47D F	5'-TGG ACG AAC TCC TCG AAC TC-3'
TpnC47D R	5'-GGT GAT CGA TCT GGT GAA CA-3'